Dark matter indirect detection from dSph galaxies and galaxy clusters: status and prospects

Céline Combet (LPSC, Grenoble)

"News from the dark", Montpellier, 05/12/2013

Introduction: DM distribution, J-factor

Dwarf spheroidal galaxies: J-factor and uncertainties

Galaxy clusters: single source vs. stacking analysis

Prospects and conclusions

CLUMPY code
Charbonnier, Combet, Maurin, CPC 183, 656 (2012)
http://lpsc.in2p3.fr/clumpy
http://lpsc.in2p3.fr/clumpy/downloads.html

Indirect detection in gamma-rays

The gamma-ray flux in given by:

$$\frac{d\Phi_\gamma}{dE_\gamma}(E_\gamma, \psi, \theta, \Delta\Omega) = \underbrace{\frac{d\Phi_\gamma^{PP}}{dE_\gamma}(E_\gamma)}_{\text{Particle physics}} \times \underbrace{J(\psi, \theta, \Delta\Omega)}_{\text{Astrophysics}}$$

Particle physics

Astrophysics

Weakly Interacting Massive Particles $m_{\text{WIMP}} \sim 0.1 - 100$ TeV

$$\frac{d\Phi_\gamma^{PP}}{dE_\gamma}(E_\gamma) \equiv \frac{1}{4\pi} \frac{\langle \sigma_{\text{ann}} v \rangle}{2m_\chi^2} \cdot \sum_f \frac{dN_\gamma^f}{dE_\gamma} B_f$$

$$J(\psi, \theta, \Delta\Omega) = \int_0^{\Delta\Omega} \int_{\text{l.o.s}} \rho^2(l(\psi, \theta)) \; dl \, d\Omega$$

Detection or non-detection

↓

J value and uncertainty must be well-known to put constraints on DM candidate

(Potential) signal depends crucially on DM distribution

Dark matter distribution: large scales

Hierarchical formation of structures in the Universe:
from micro-haloes to galaxy clusters

Galaxy clusters are the largest gravitationnally-bound structures in the universe, $M \sim 10^{14} - 10^{15}\ M_{sun}$

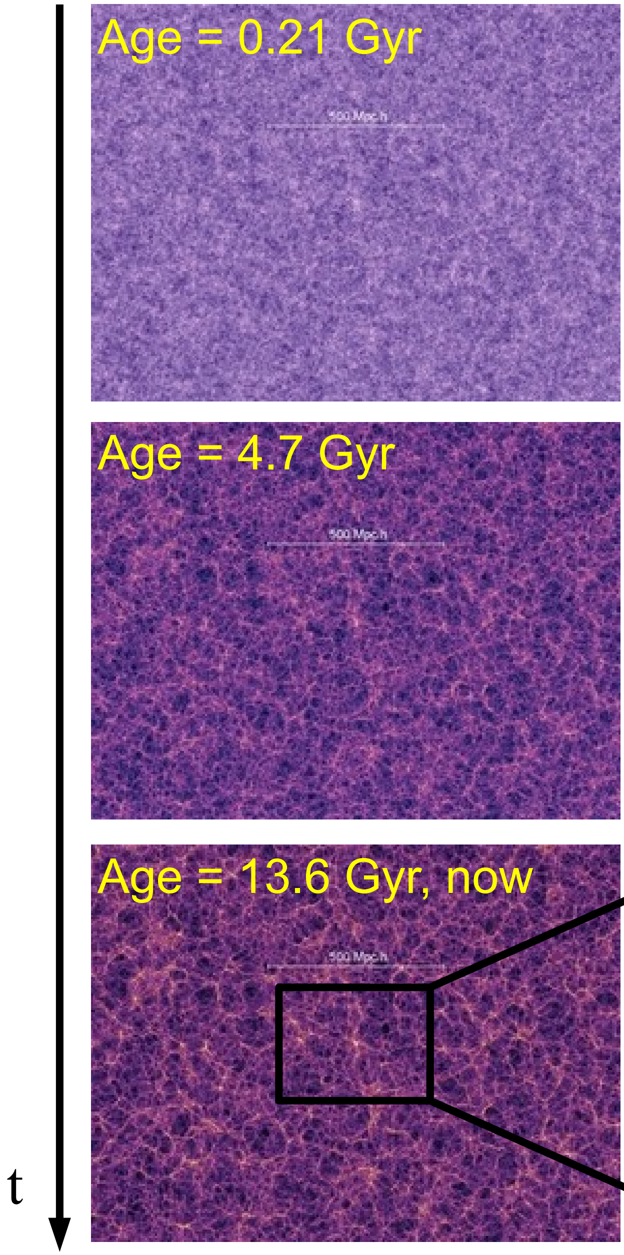

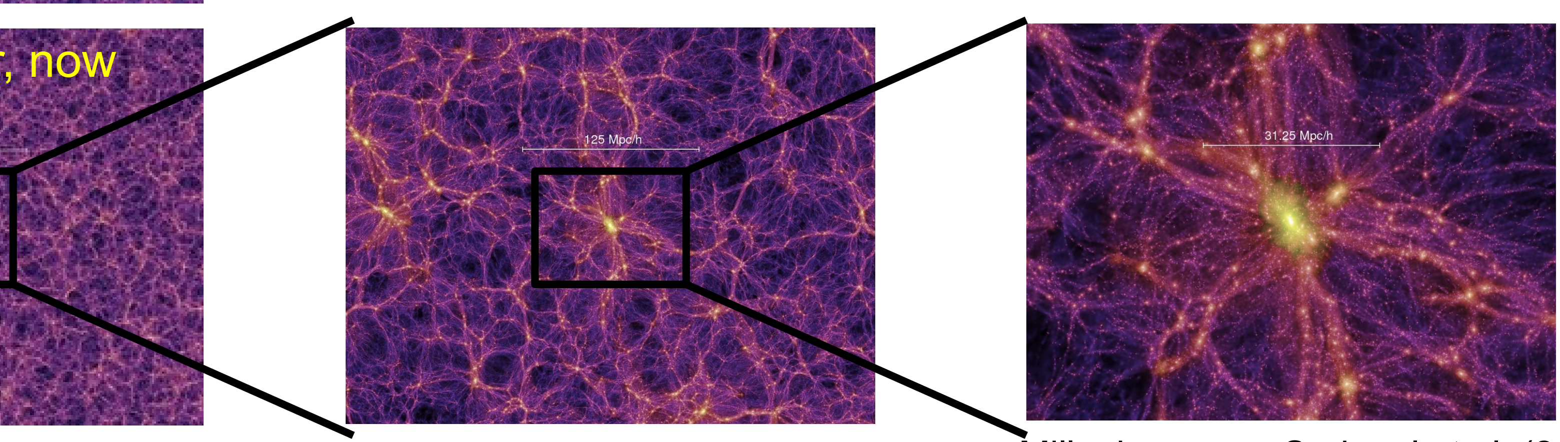

Millenium run – Springel et al. (2005)

Dark matter distribution: Galactic scale

Aquarius (MW-like) simulation – Springel et al (2008)

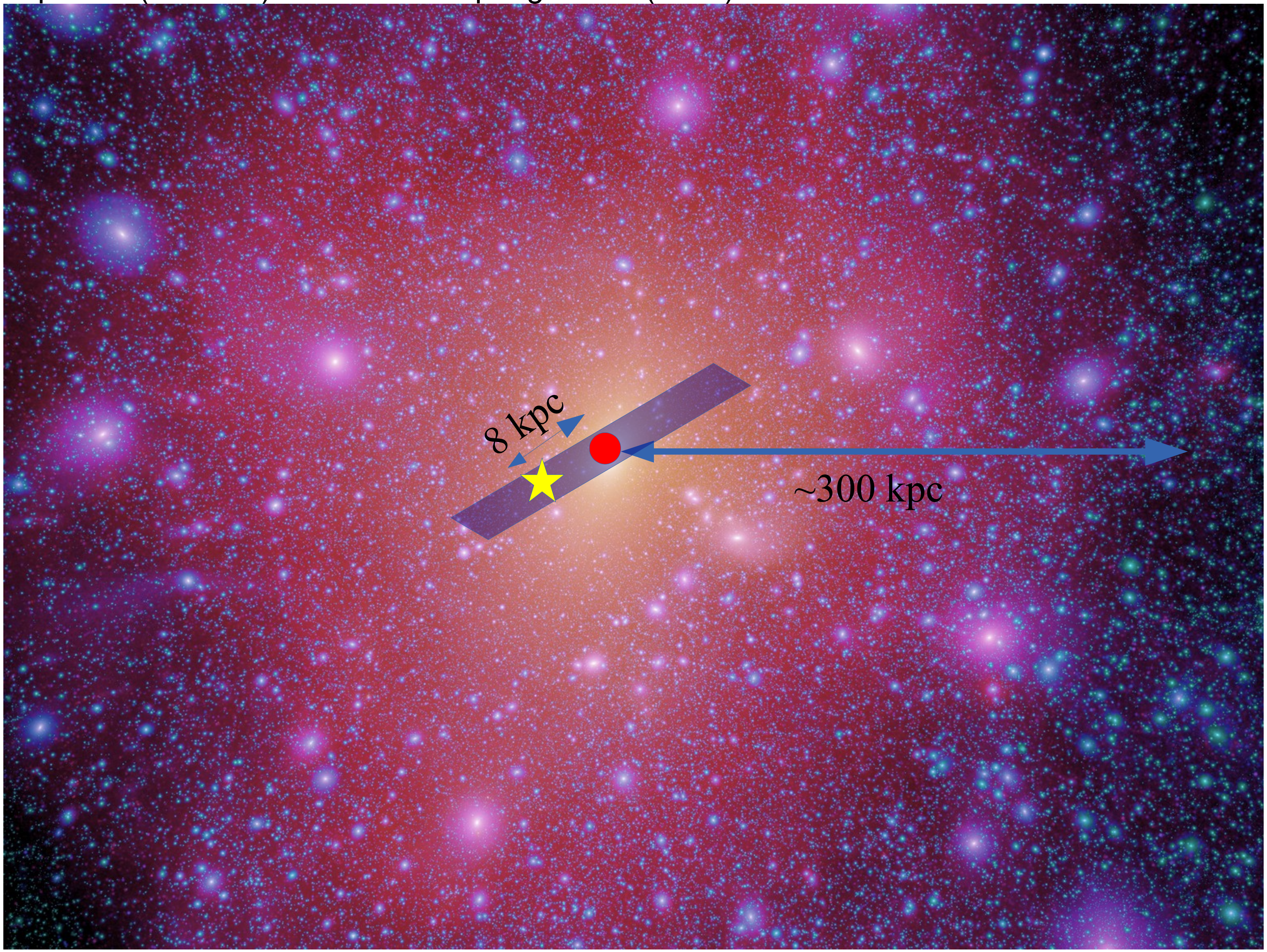

Where to look?

Dense ($\sim \int \rho^2$) – Close ($1/d^2$) – No astrophysical background

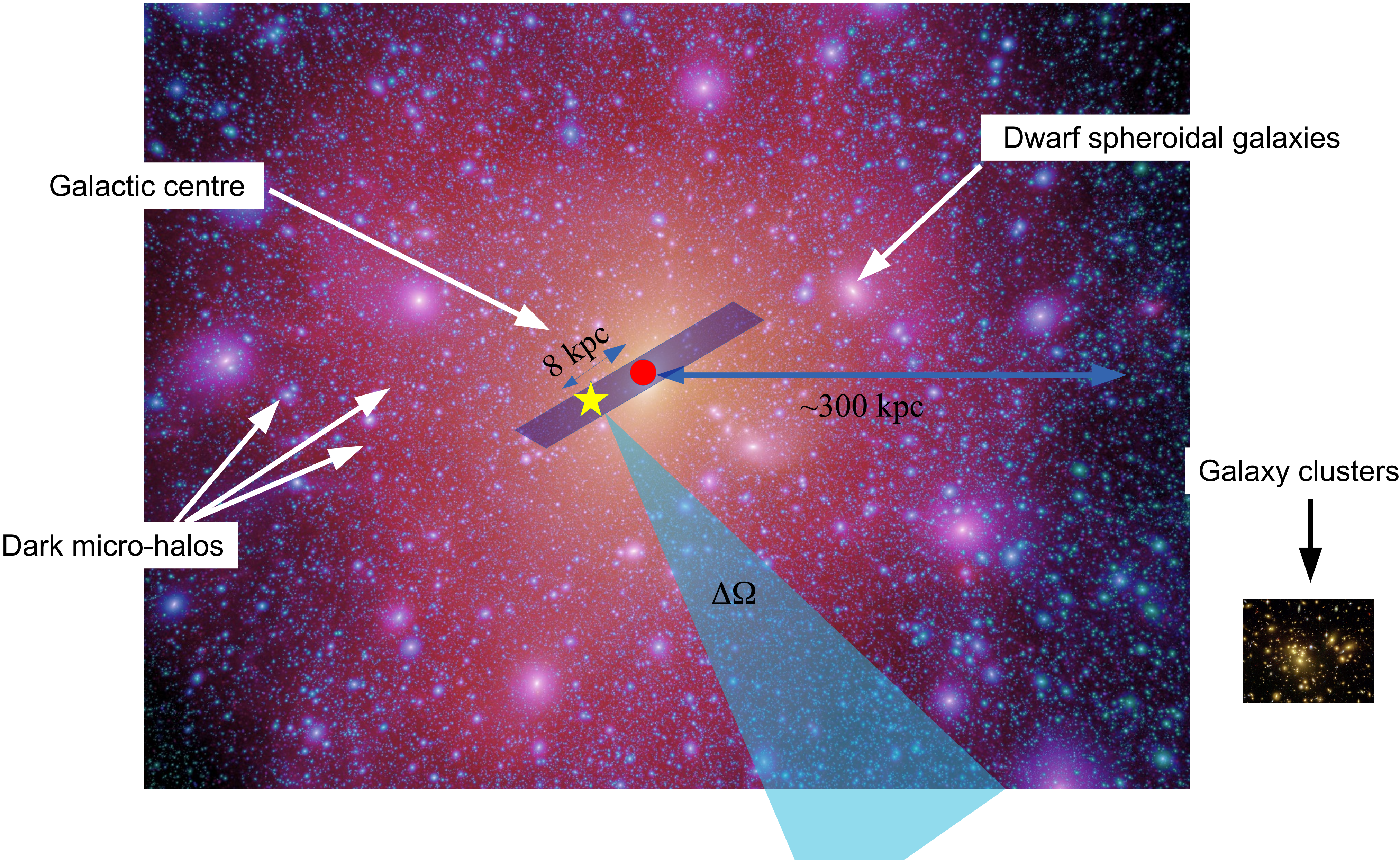

J_{tot}, substructures, and boost factor

$$J = \int_0^{\Delta\Omega} \int_{l_{\min}}^{l_{\max}} \frac{1}{l^2} \left(\rho_{\rm sm} + \sum_i \rho_{\rm cl}^i \right)^2 l^2 dl d\Omega$$

[up to 20% of J_{tot} in some config.]

[boost signal]

$$J_{\rm sm} \equiv \int_0^{\Delta\Omega} \int_{l_{\min}}^{l_{\max}} \rho_{\rm sm}^2 dl d\Omega$$

$$J_{\rm cross-prod} \equiv 2 \int_0^{\Delta\Omega} \int_{l_{\min}}^{l_{\max}} \rho_{\rm sm} \sum_i \rho_{\rm cl}^i dl d\Omega$$

$$J_{\rm subs} \equiv \int_0^{\Delta\Omega} \int_{l_{\min}}^{l_{\max}} \left(\sum_i \rho_{\rm cl}^i \right)^2 dl d\Omega$$

J_{tot}, substructures, and boost factor

$$J = \int_0^{\Delta\Omega}\int_{l_{\rm min}}^{l_{\rm max}} \frac{1}{l^2}\left(\rho_{\rm sm} + \sum_i \rho_{\rm cl}^i\right)^2 l^2 dl d\Omega$$

$$J_{\rm sm} \equiv \int_0^{\Delta\Omega}\int_{l_{\rm min}}^{l_{\rm max}} \rho_{\rm sm}^2 dl d\Omega$$

[up to 20% of J_{tot} in some config.]

$$J_{\rm cross-prod} \equiv 2\int_0^{\Delta\Omega}\int_{l_{\rm min}}^{l_{\rm max}} \rho_{\rm sm}\sum_i \rho_{\rm cl}^i dl d\Omega$$

[boost signal]

$$J_{\rm subs} \equiv \int_0^{\Delta\Omega}\int_{l_{\rm min}}^{l_{\rm max}} \left(\sum_i \rho_{\rm cl}^i\right)^2 dl d\Omega$$

[exact realisation (mass and position) of DM distribution unknown]

Average description

$$\langle J_{\rm cross-prod}\rangle = 2\int_0^{\Delta\Omega}\int_{l_{\rm min}}^{l_{\rm max}} \rho_{\rm sm}\langle\rho_{\rm subs}\rangle dl d\Omega$$

$$\langle J_{\rm subs}\rangle = N_{\rm tot}\int_0^{\Delta\Omega}\int_{l_{\rm min}}^{l_{\rm max}} \frac{d\mathcal{P}_V}{dV} dl d\Omega \int_{M_{\rm min}}^{M_{\rm max}} \mathcal{L}(M)\frac{\mathcal{P}_M}{dM} dM$$

$$\mathcal{L}(M) \equiv \int_{\rm V_{cl}} (\rho_{\rm cl})^2 dV$$

J_{tot}, substructures, and boost factor

Angular dependence – integration along the l.o.s

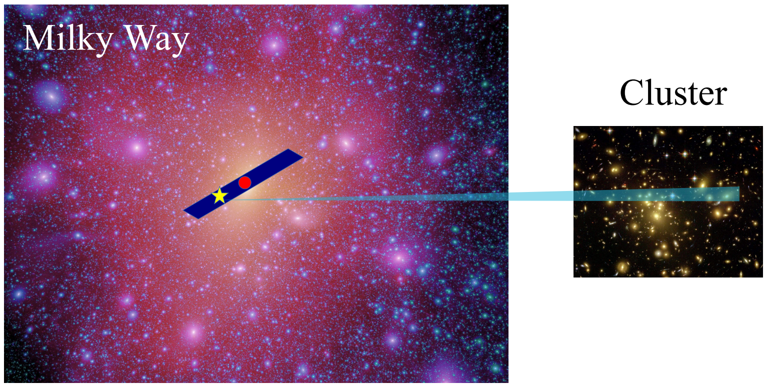

Smooth (involves $\rho_{\rm sm}^2$)

$$\frac{dJ_{\rm sm}}{d\Omega}(\theta) = \int_{l_{\rm min}}^{l_{\rm max}} \rho_{\rm sm}^2 dl$$

→ peaked near centre

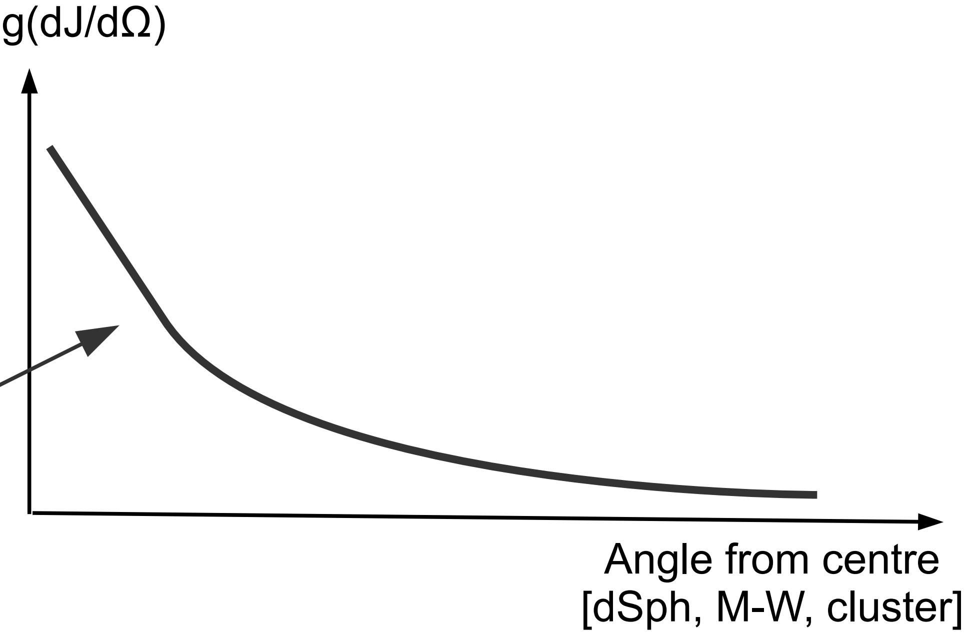

J_{tot}, substructures, and boost factor

Angular dependence – integration along the l.o.s

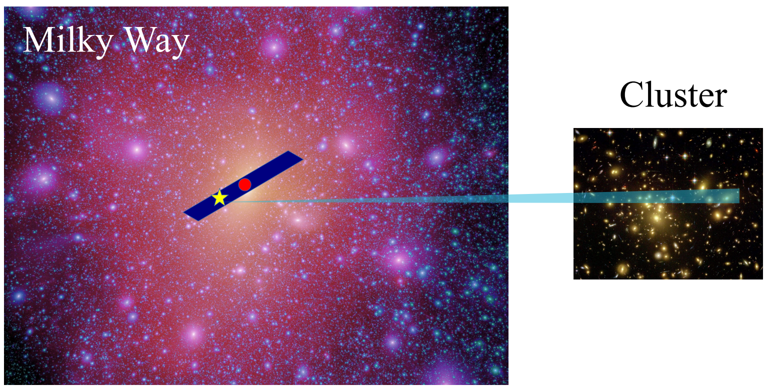

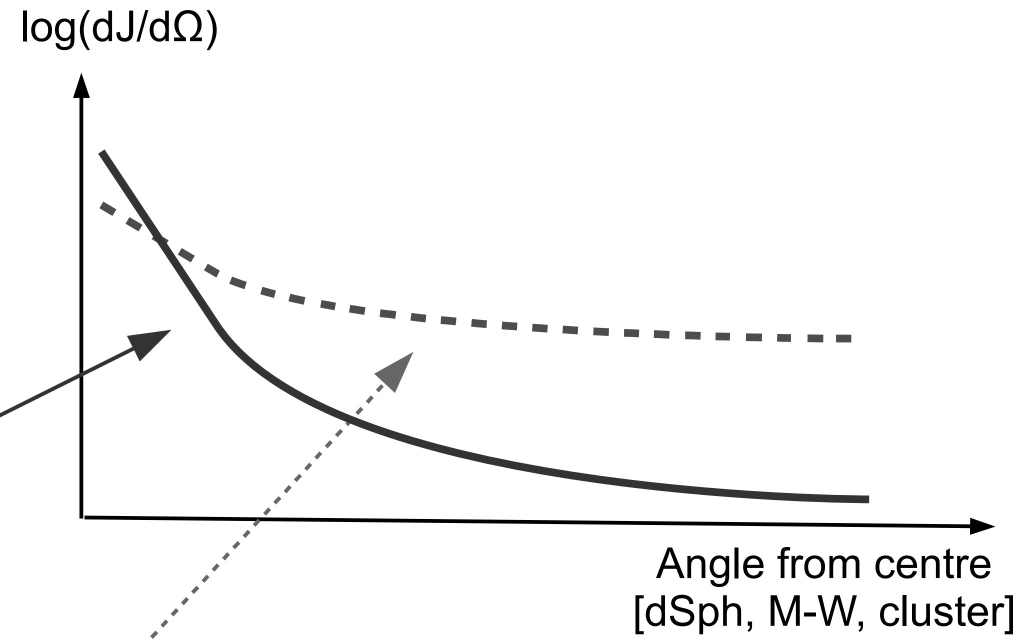

Smooth (involves $\rho_{\rm sm}^2$)

$$\frac{dJ_{\rm sm}}{d\Omega}(\theta) = \int_{l_{\rm min}}^{l_{\rm max}} \rho_{\rm sm}^2 dl$$

→ peaked near centre

Subs (involves $\rho_{\rm sub}$)

N.B.: spat. dist. flatter than $\rho_{\rm sm}$ (near centre)

$$\langle \frac{dJ_{\rm sub}}{d\Omega}(\theta) \rangle = N_{\rm tot} \int_{l_{\rm min}}^{l_{\rm max}} \frac{d\mathcal{P}_{\mathcal{V}}}{dV} \int_{M_{\rm min}}^{M_{\rm max}} \mathcal{L}(M) \frac{d\mathcal{P}_{\mathcal{M}}}{dM} dM$$

→ less peaked (centre), shallower decrease

J_{tot}, substructures, and boost factor

Signal boost from substructures (α_{int} vs R_{vir}/d)

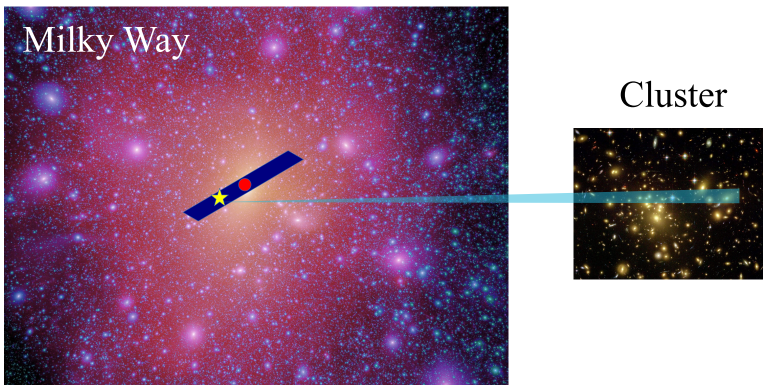

Smooth (involves ρ^2_{sm})

$$\frac{dJ_{sm}}{d\Omega}(\theta) = \int_{l_{min}}^{l_{max}} \rho^2_{sm} dl$$

→ peaked near centre

Subs (involves ρ_{sub})

N.B.: spat. dist. flatter than ρ_{sm} (near centre)

$$\langle \frac{dJ_{sub}}{d\Omega}(\theta) \rangle = N_{tot} \int_{l_{min}}^{l_{max}} \frac{d\mathcal{P}_V}{dV} \int_{M_{min}}^{M_{max}} \mathcal{L}(M) \frac{d\mathcal{P}_M}{dM} dM$$

→ less peaked (centre), shallower decrease

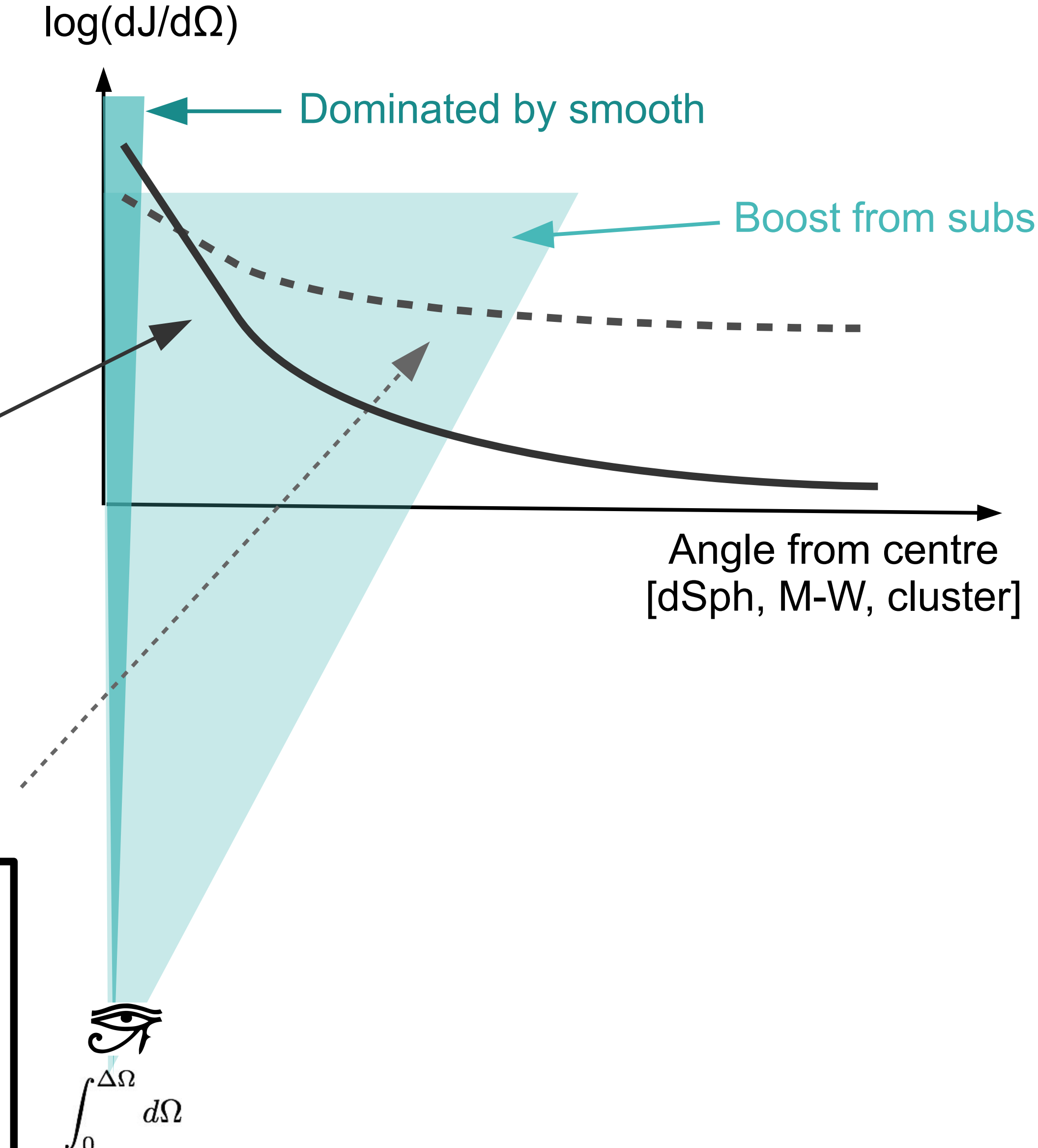

J_{tot}, substructures, and boost factor

Signal boost from substructures (α_{int} vs R_{vir}/d)

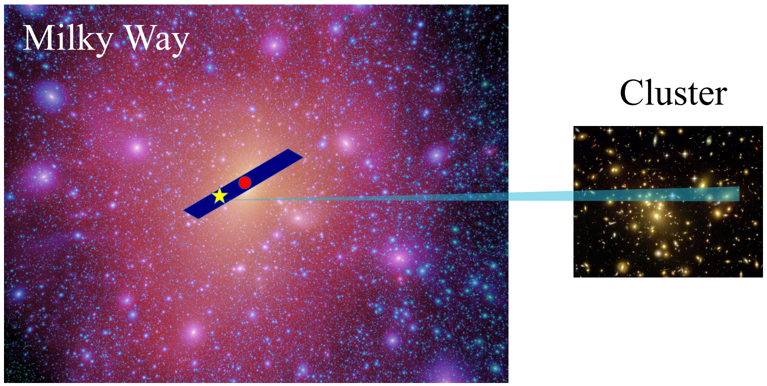

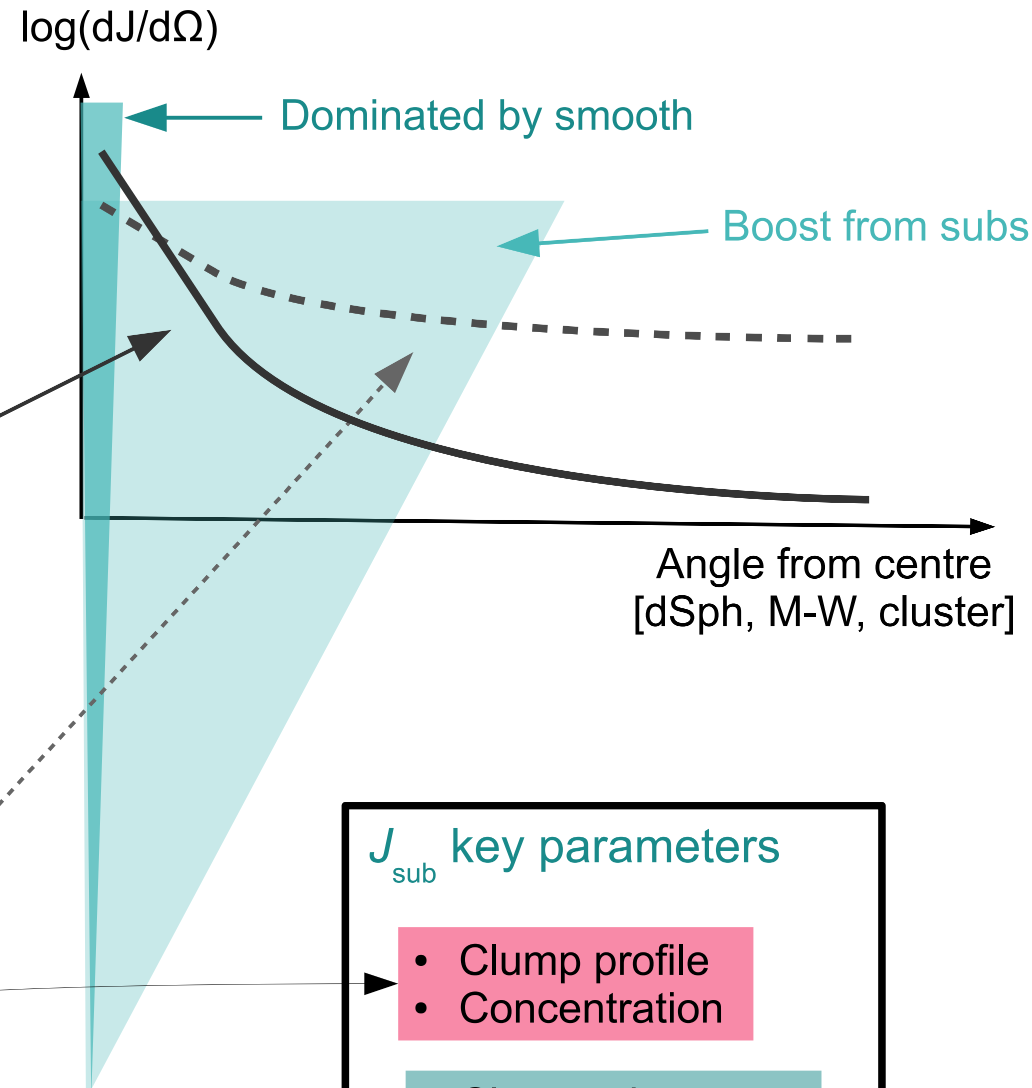

Smooth (involves $\rho_{\rm sm}^2$)

$$\frac{dJ_{\rm sm}}{d\Omega}(\theta) = \int_{l_{\rm min}}^{l_{\rm max}} \rho_{\rm sm}^2 dl$$

→ peaked near centre

Subs (involves $\rho_{\rm sub}$)

N.B.: spat. dist. flatter than $\rho_{\rm sm}$ (near centre)

$$\langle\frac{dJ_{\rm sub}}{d\Omega}(\theta)\rangle = N_{\rm tot} \int_{l_{\rm min}}^{l_{\rm max}} \frac{d\mathcal{P}_V}{dV} \int_{M_{\rm min}}^{M_{\rm max}} \mathcal{L}(M) \frac{d\mathcal{P}_M}{dM} dM$$

→ less peaked (centre), shallower decrease

J_{sub} key parameters

- Clump profile
- Concentration

- Clump min. mass
- Mass distribution

Introduction: DM distribution, J-factor

Dwarf spheroidal galaxies: J-factor and uncertainties

Galaxy clusters: single source vs. stacking analysis

Prospects and conclusions

Optimal integration angle: Walker et al., ApJL 733, 46 (2011)
Classical dSphs and Fermi-LAT/CTA: Charbonnier et al., MNRAS 418, 1526 (2011)

[N.B.: J not boosted for dSphs]

8 classical dSph galaxies (before SDSS)

Brightest of the MW's satellites ('plenty' of kinematic data)

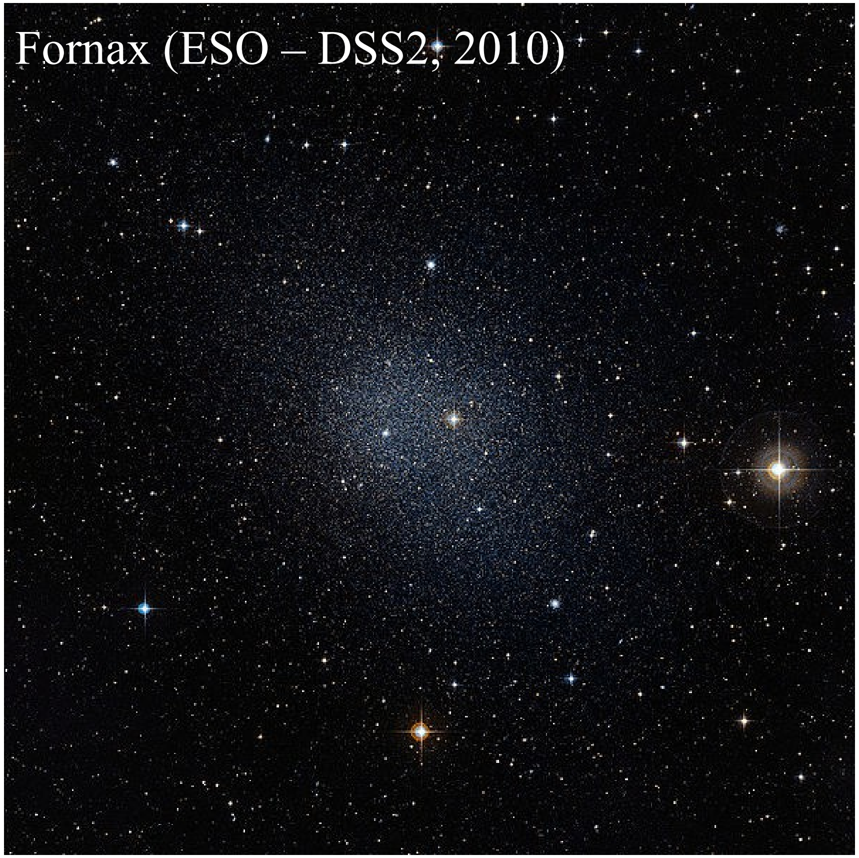

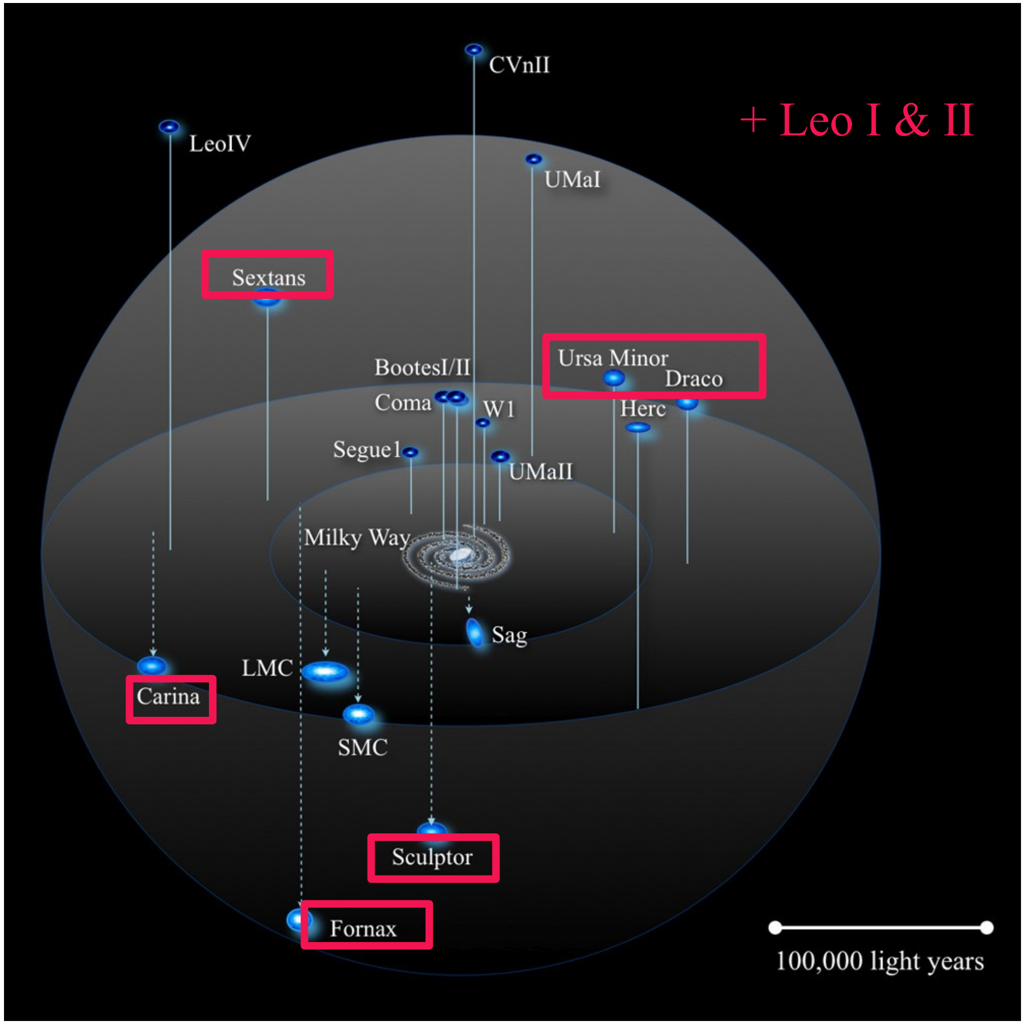

→ Dominated by DM ($m_{stars} << m_{DM} \sim 10^7\, M_{sun}$)

→ No expected γ-ray background emission

From stellar kinematics to DM profile

- **Light profile and velocity dispersion**

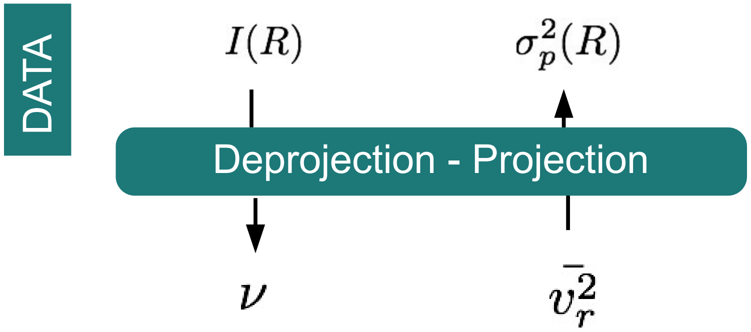

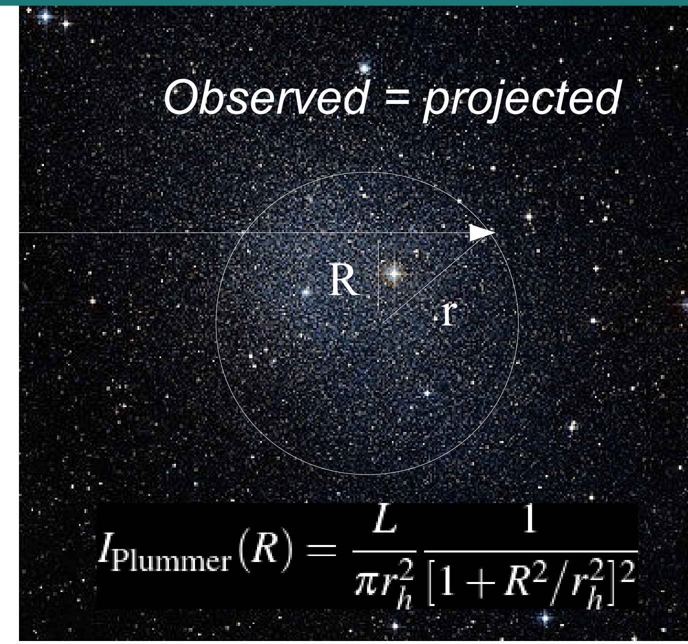

From stellar kinematics to DM profile

- **Light profile and velocity dispersion**

DATA

$I(R)$ → Deprojection - Projection → ν

$\overline{v_r^2}$ → Deprojection - Projection → $\sigma_p^2(R)$

- **Jeans equation: solve for $\overline{v_r^2}$**

MODEL

Stellar density — *Radial velocity dispersion*

$$\frac{1}{\nu}\frac{d}{dr}(\nu\overline{v_r^2}) + 2\frac{\beta_{\rm ani}\overline{v_r^2}}{r} = -\frac{GM(r)}{r^2}$$

Anisotropy — *Enclosed mass*

$$\beta_{\rm ani} = 1 - \overline{v_\theta^2}/\overline{v_r^2} \qquad M(r) = \int_0^r 4\pi s^2 \rho(s) ds$$

Collisionless Boltzman
Spherical symmetry

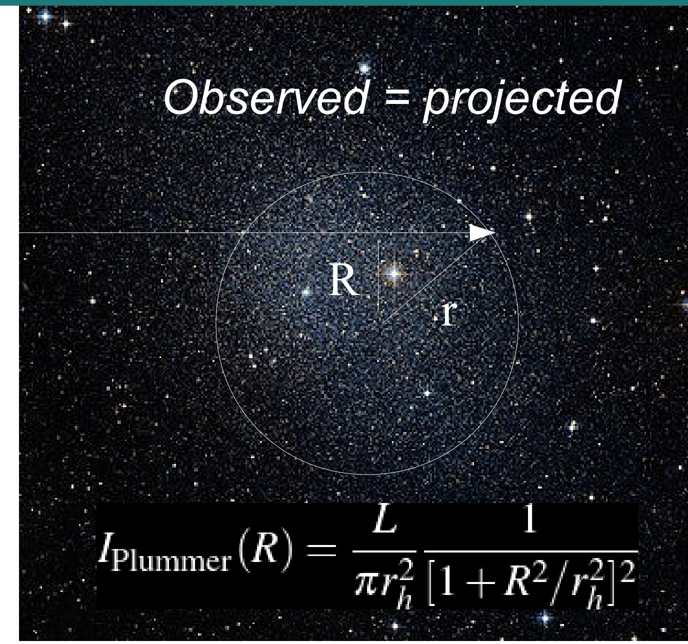

From stellar kinematics to DM profile

DATA

- **Light profile and velocity dispersion**

$I(R)$ → Deprojection - Projection → ν

$\overline{v_r^2}$ → Deprojection - Projection → $\sigma_p^2(R)$

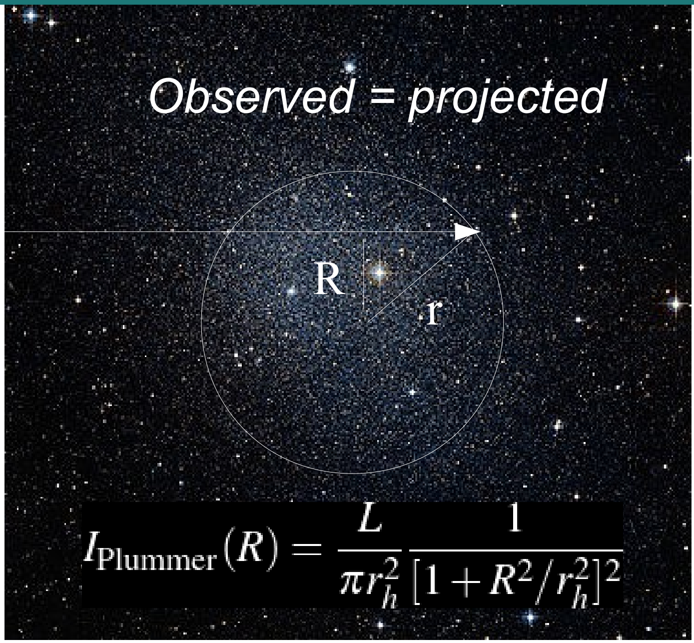

MODEL

- **Jeans equation: solve for $\overline{v_r^2}$**

Stellar density, *Radial velocity dispersion*

$$\frac{1}{\nu}\frac{d}{dr}(\nu \overline{v_r^2}) + 2\frac{\beta_{\rm ani}\overline{v_r^2}}{r} = -\frac{GM(r)}{r^2}$$

Collisionless Boltzman
Spherical symmetry

Anisotropy

$$\beta_{\rm ani} = 1 - \overline{v_\theta^2}/\overline{v_r^2}$$

Enclosed mass

$$M(r) = \int_0^r 4\pi s^2 \rho(s) ds$$

FREE PAR.

- **Dark matter profile**

$$\rho(r) = \frac{\rho_s}{\left(\frac{r}{r_s}\right)^\gamma \left[1 + \left(\frac{r}{r_s}\right)^\alpha\right]^{(\beta-\gamma)/\alpha}}$$

$$\rho_s,\ r_s,\ \alpha,\ \beta,\ \gamma,\ (\text{and } \beta_{\rm ani})$$

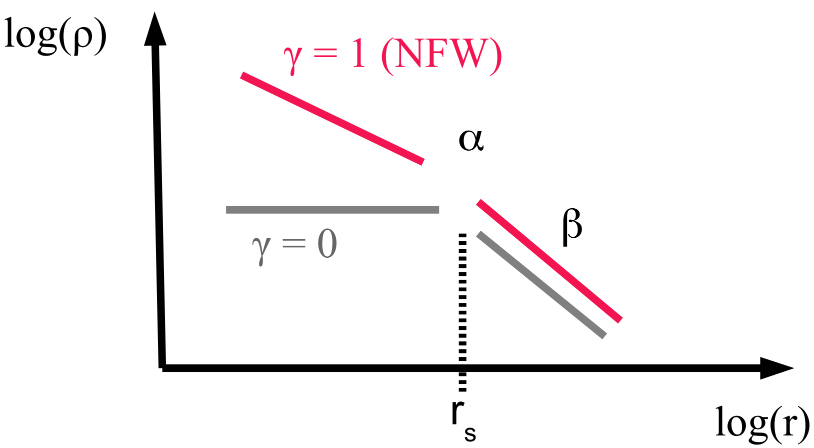

From stellar kinematics to DM profile

DATA

- **Light profile and velocity dispersion**

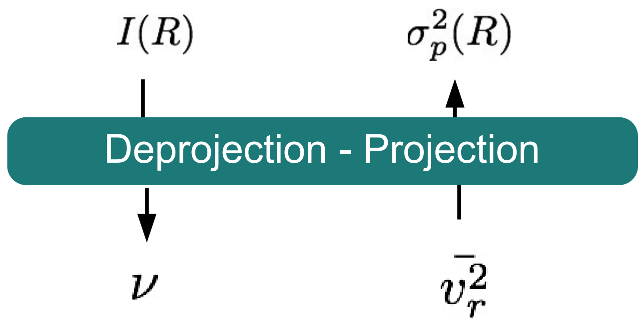

MODEL

- **Jeans equation: solve for $\bar{v_r^2}$**

Stellar density — *Radial velocity dispersion*

$$\frac{1}{\nu}\frac{d}{dr}(\nu\bar{v_r^2}) + 2\frac{\beta_{\rm ani}\bar{v_r^2}}{r} = -\frac{GM(r)}{r^2}$$

Anisotropy — *Enclosed mass*

$$\beta_{\rm ani} = 1 - \bar{v_\theta^2}/\bar{v_r^2} \qquad M(r) = \int_0^r 4\pi s^2 \rho(s) ds$$

FREE PARAM.

- **Dark matter profile**

$$\rho(r) = \frac{\rho_s}{\left(\frac{r}{r_s}\right)^\gamma \left[1 + \left(\frac{r}{r_s}\right)^\alpha\right]^{(\beta-\gamma)/\alpha}}$$

$$\rho_s,\ r_s,\ \alpha,\ \beta,\ \gamma,\ (\text{and } \beta_{\rm ani})$$

Best fit on velocity dispersion data (^{2} analysis)

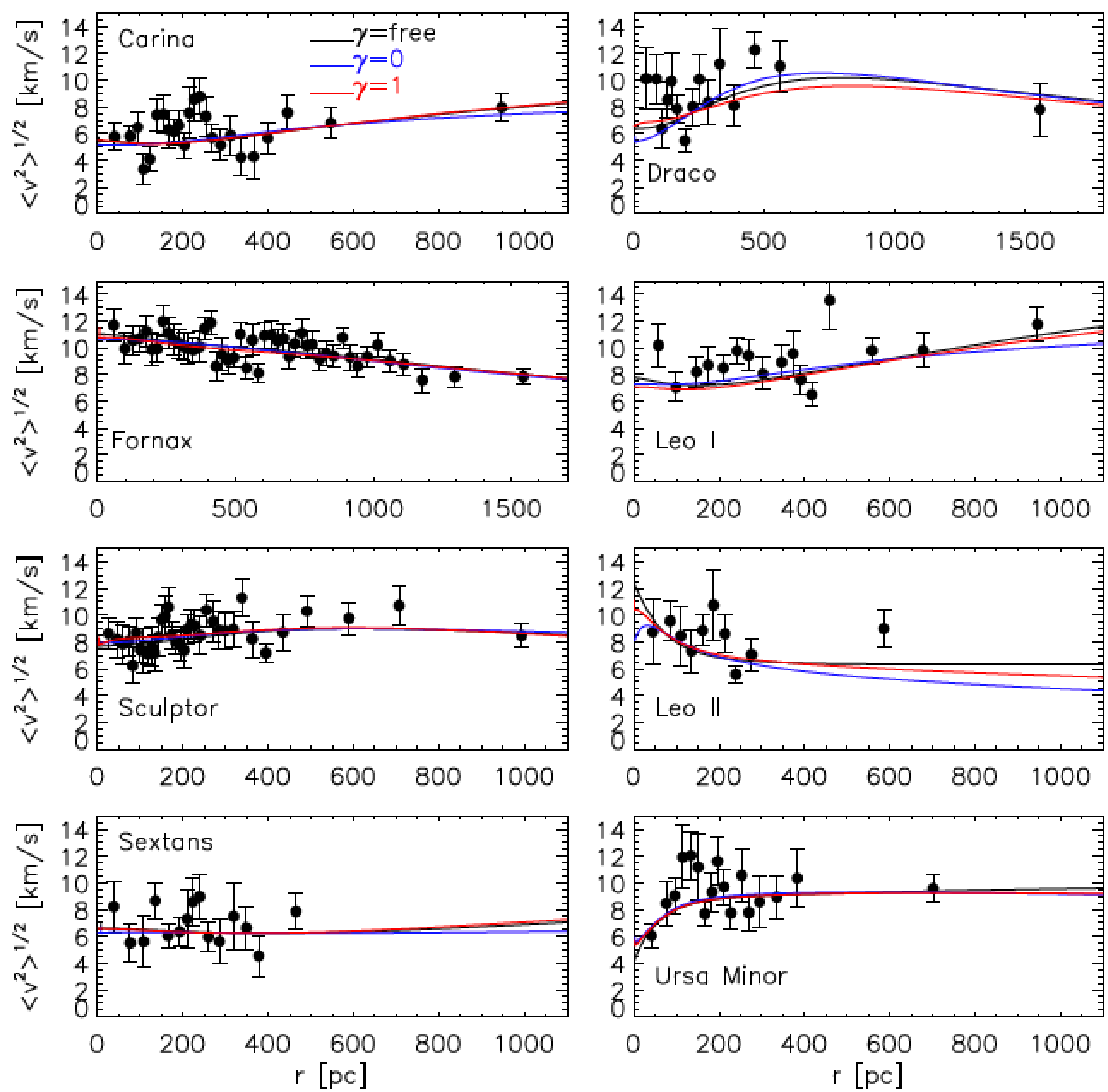

Not sensitive to the inner slope

From stellar kinematics to DM profile

DATA

- **Light profile and velocity dispersion**

$I(R)$ $\sigma_p^2(R)$

Deprojection - Projection

ν $\bar{v_r^2}$

- **Jeans equation: solve for** $\bar{v_r^2}$

MODEL

Stellar density *Radial velocity dispersion*

$$\frac{1}{\nu}\frac{d}{dr}(\nu \bar{v_r^2}) + 2\frac{\beta_{\rm ani}\bar{v_r^2}}{r} = -\frac{GM(r)}{r^2}$$

Anisotropy *Enclosed mass*

$$\beta_{\rm ani} = 1 - \bar{v_\theta^2}/\bar{v_r^2} \qquad M(r) = \int_0^r 4\pi s^2 \rho(s) ds$$

- **Dark matter profile**

FREE PARAM.

$$\rho(r) = \frac{\rho_s}{\left(\frac{r}{r_s}\right)^\gamma \left[1 + \left(\frac{r}{r_s}\right)^\alpha\right]^{(\beta-\gamma)/\alpha}}$$

$$\rho_s,\ r_s,\ \alpha,\ \beta,\ \gamma,\ (\text{and } \beta_{\rm ani})$$

Parameter space sampling (Markov Chain Monte Carlo)

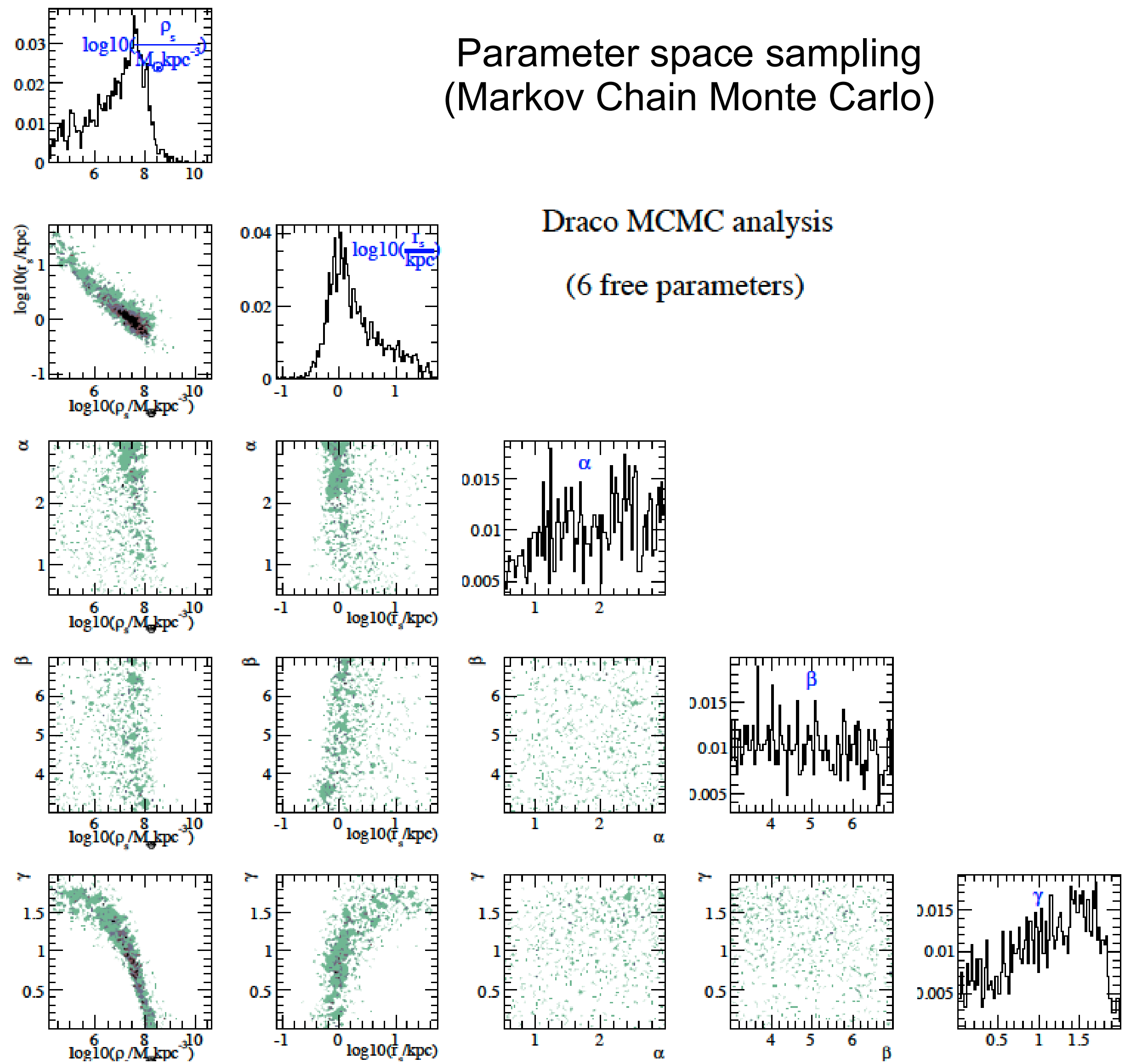

Draco MCMC analysis

(6 free parameters)

Recover median and CLs on any quantity (e.g., J)

Optimal integration angle

$$J = \int_0^{2\pi} \int_0^{\alpha_{\rm int}} \int_0^{\infty} \rho_{\rm sm}^2 \, dl \, d\alpha \, d\beta$$

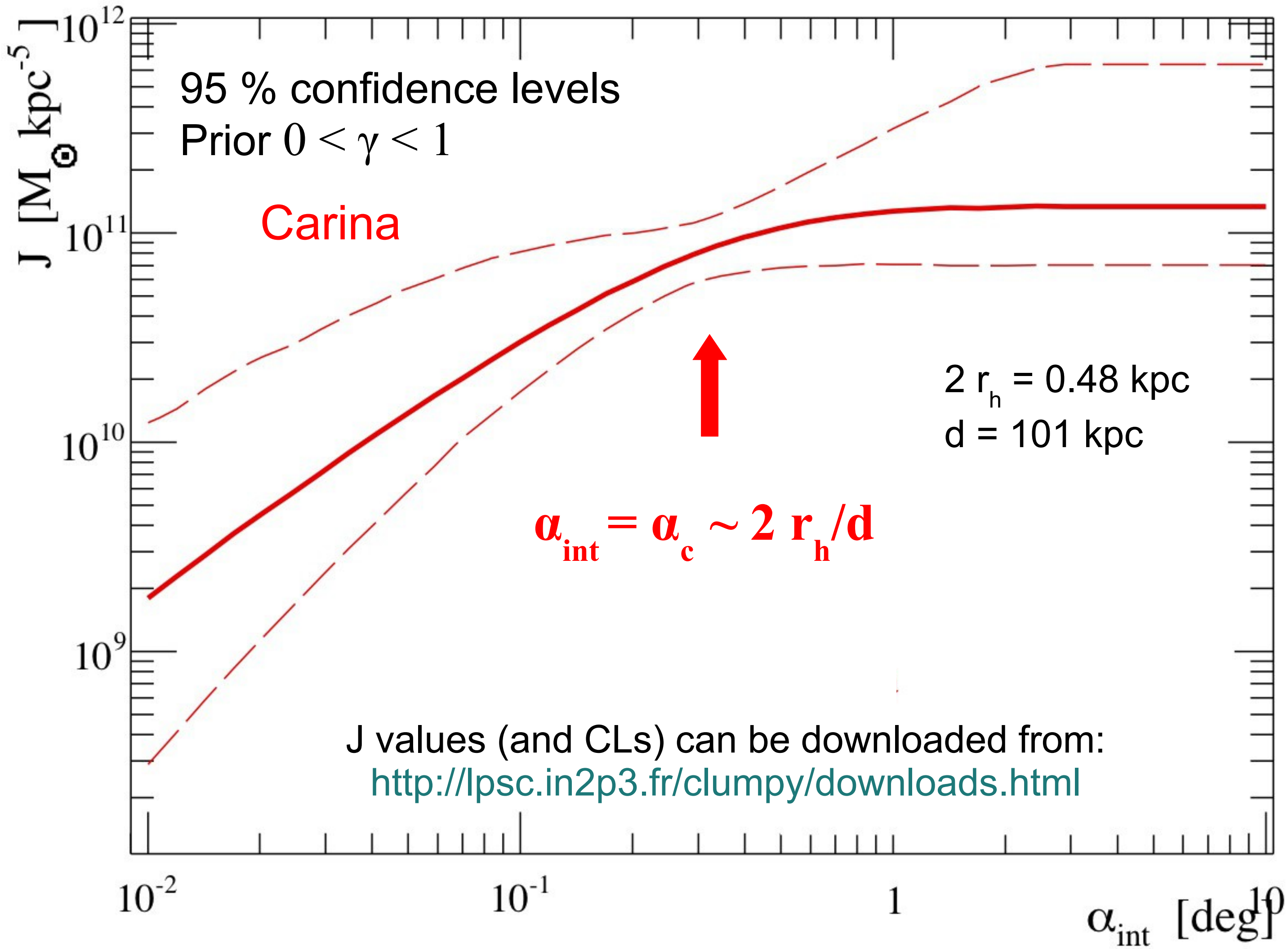

Optimal integration angle

$$J = \int_0^{2\pi} \int_0^{\alpha_{\rm int}} \int_0^{\infty} \rho_{\rm sm}^2 \, dl \, d\alpha \, d\beta$$

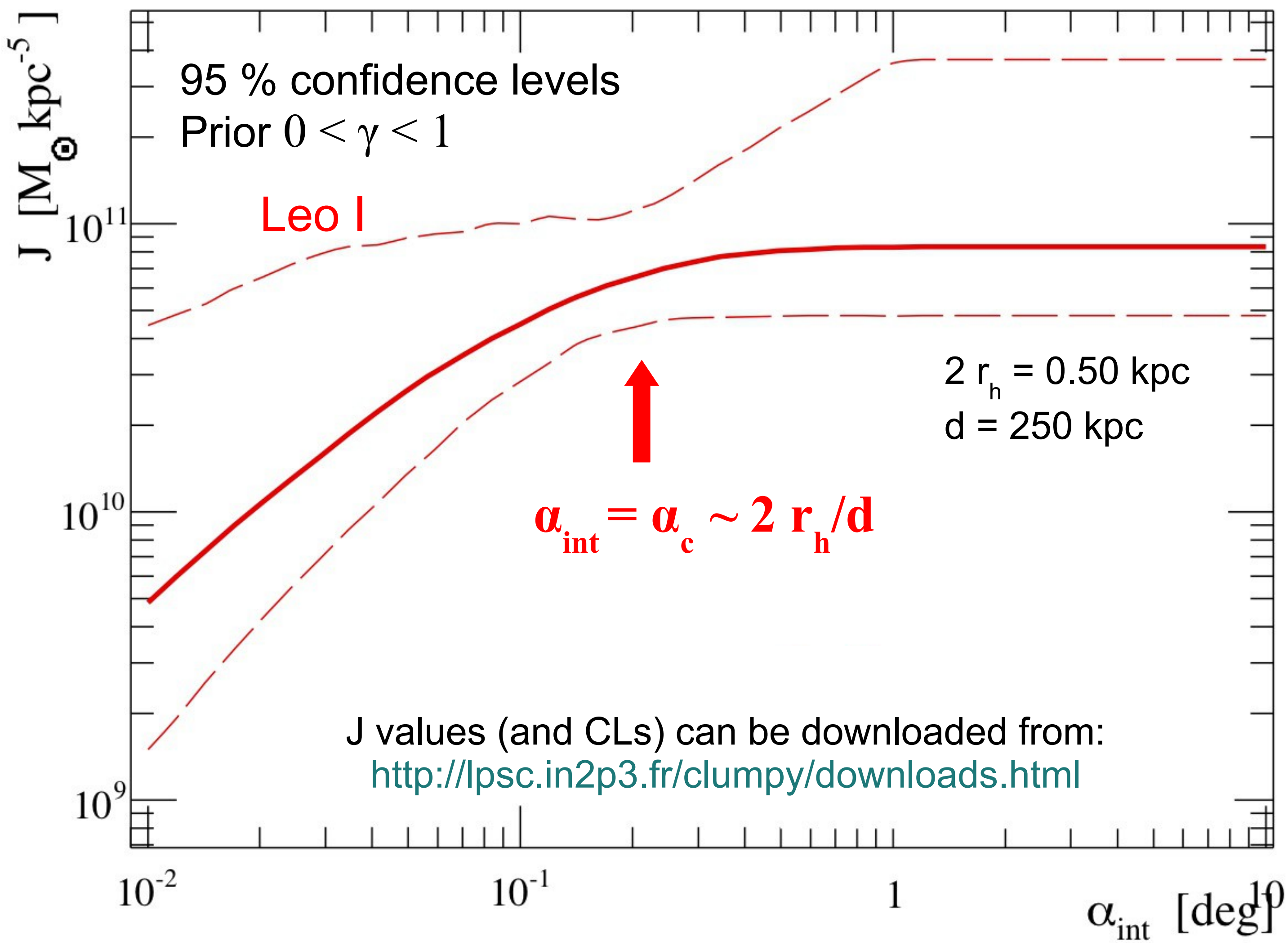

Ranking and contrast

$$J = \int_0^{2\pi} \int_0^{\alpha_{\rm int}} \int_0^{\infty} \rho_{\rm sm}^2 \; dl \, d\alpha \, d\beta$$

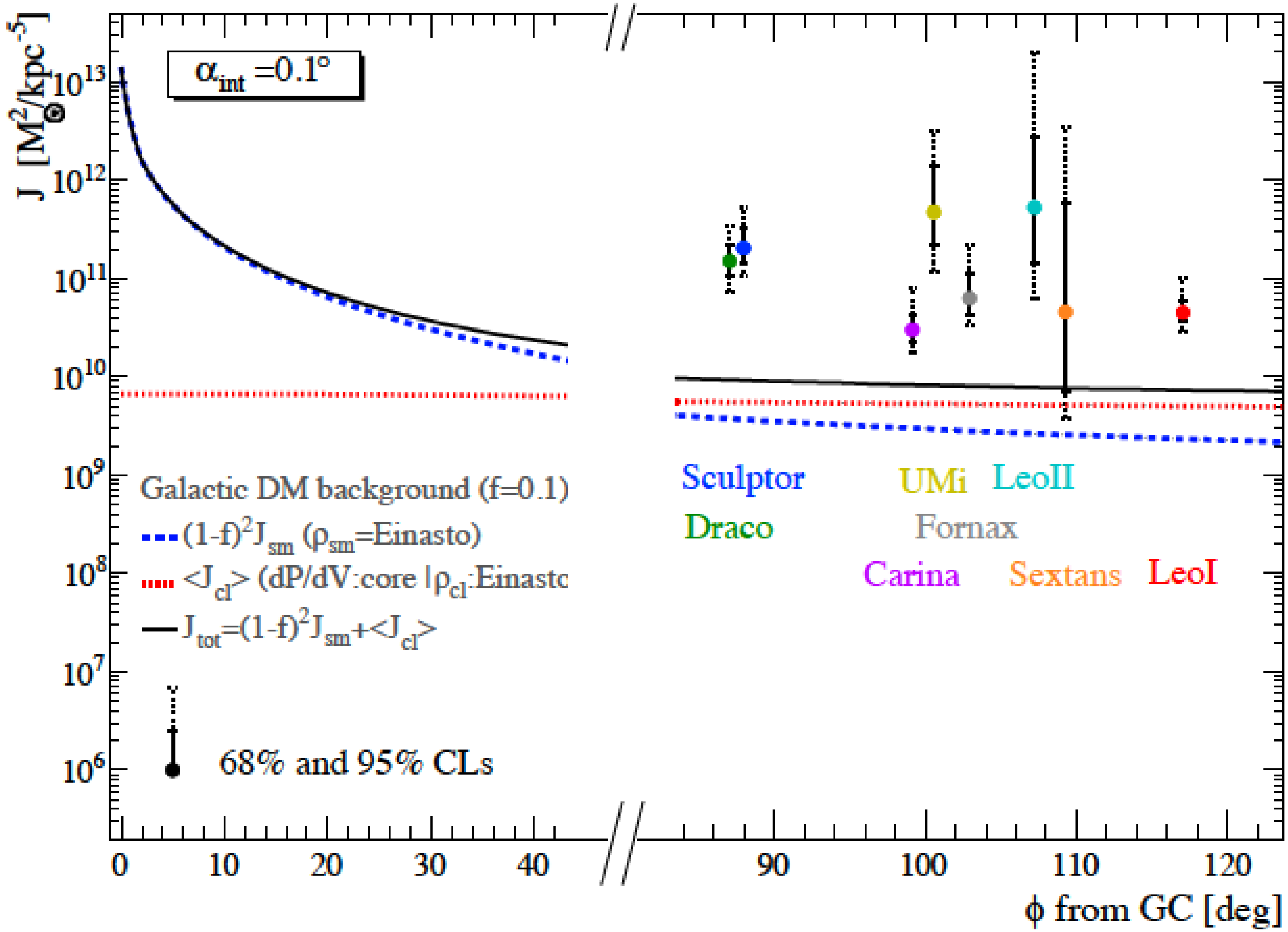

$$J_{\rm bckg} \propto \alpha_{\rm int}^2$$

- Best targets: Draco, Sculptor, (and UMi ?)

Ranking and contrast

$$J = \int_0^{2\pi} \int_0^{\alpha_{\rm int}} \int_0^{\infty} \rho_{\rm sm}^2 \; dl \, d\alpha \, d\beta$$

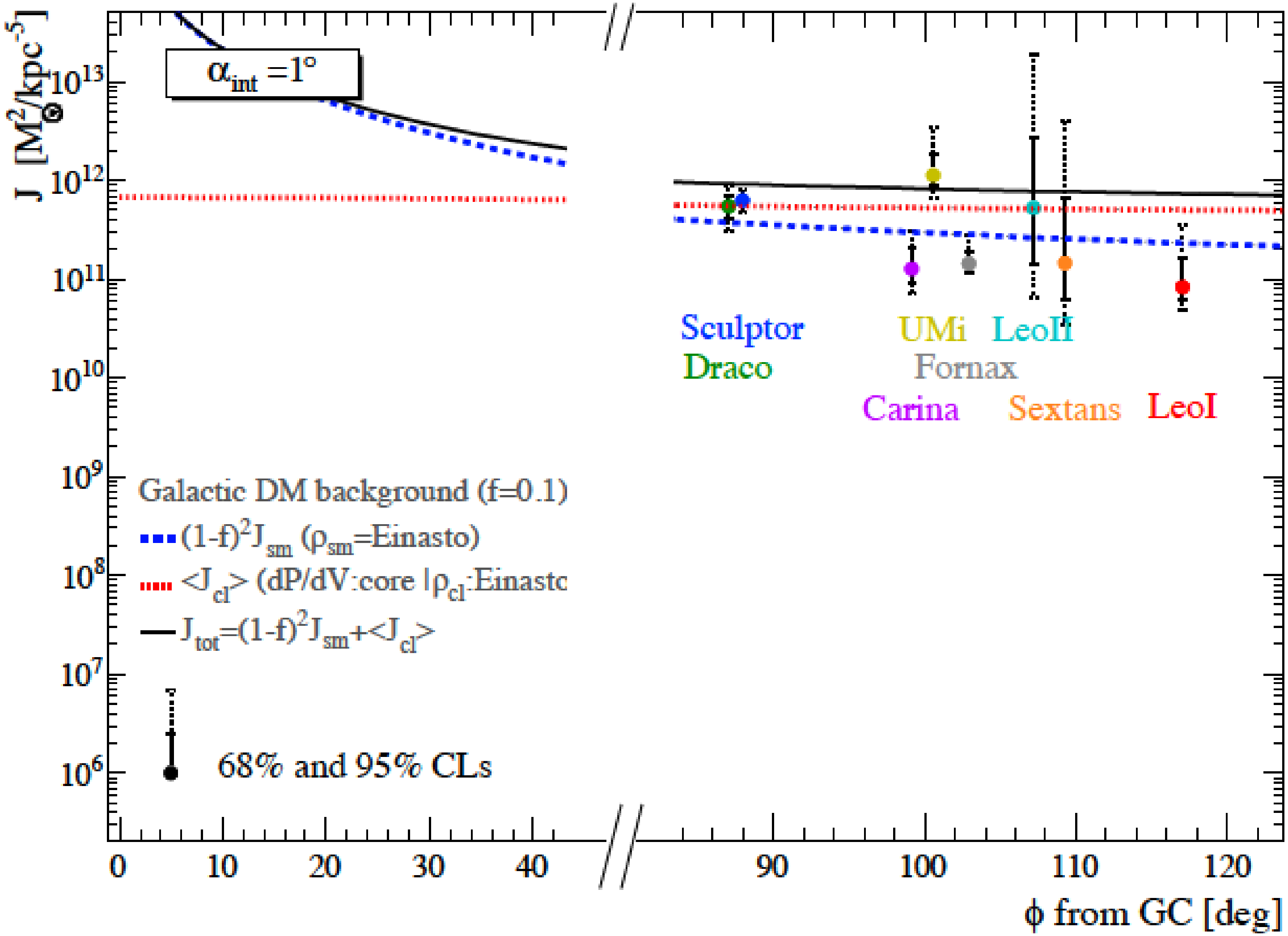

$$J_{\rm bckg} \propto \alpha_{\rm int}^2$$

$$\frac{J_{\rm bckg}(1^\circ)}{J_{\rm bckg}(0.1^\circ)} \sim 10^2$$

$$\frac{J_{\rm dSph}(1^\circ)}{J_{\rm dSph}(0.1^\circ)} \sim \text{a few}$$

- Best targets: Draco, Sculptor, (and UMi ?)
- For instruments with α_{int}~1°, change strategy

Limit on annihilation cross-section

$$\underbrace{\frac{d\Phi_\gamma}{dE_\gamma}(E_\gamma,\psi,\theta,\Delta\Omega)}_{\text{Instrumental sensitivity}} = \underbrace{\frac{d\Phi_\gamma^{PP}}{dE_\gamma}(E_\gamma)}_{\text{Particle physics}} \times \underbrace{J(\psi,\theta,\Delta\Omega)}_{\text{Constrained}}$$

Instrumental sensitivity → **IACT** / **Satellite**

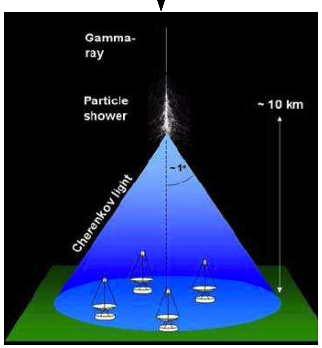

HESS, MAGIC, VERITAS

CTA (~2016-2020)

- Ground based
- 100 GeV → 100 TeV
- Resolution: 0.2° – 0.02°
- CR contamination
  → background limited

Fermi-LAT

- Space-borne
- 30 MeV – 300 GeV
- Resolution: 1° – 0.1°
- Fullsky

Limit on annihilation cross-section

$$\frac{d\Phi_\gamma}{dE_\gamma}(E_\gamma,\psi,\theta,\Delta\Omega) = \frac{d\Phi_\gamma^{PP}}{dE_\gamma}(E_\gamma) \times J(\psi,\theta,\Delta\Omega)$$

Instrumental sensitivity — Particle physics — Constrained

Instrumental sensitivity: IACT / Satellite

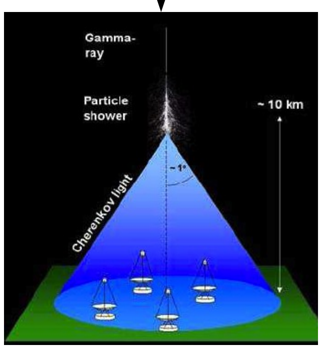

HESS, MAGIC, VERITAS

CTA (~2016-2020)

- Ground based
- 100 GeV → 100 TeV
- Resolution: 0.2° – 0.02°
- CR contamination → background limited

Fermi-LAT

- Space-borne
- 30 MeV – 300 GeV
- Resolution: 1° – 0.1°
- Fullsky

Particle physics:

$$\frac{d\Phi_\gamma^{PP}}{dE_\gamma}(E_\gamma) \equiv \frac{1}{4\pi}\,\frac{\langle\sigma_{\rm ann}v\rangle}{2m_\chi^2}\cdot\sum_f \frac{dN_\gamma^f}{dE_\gamma}B_f$$

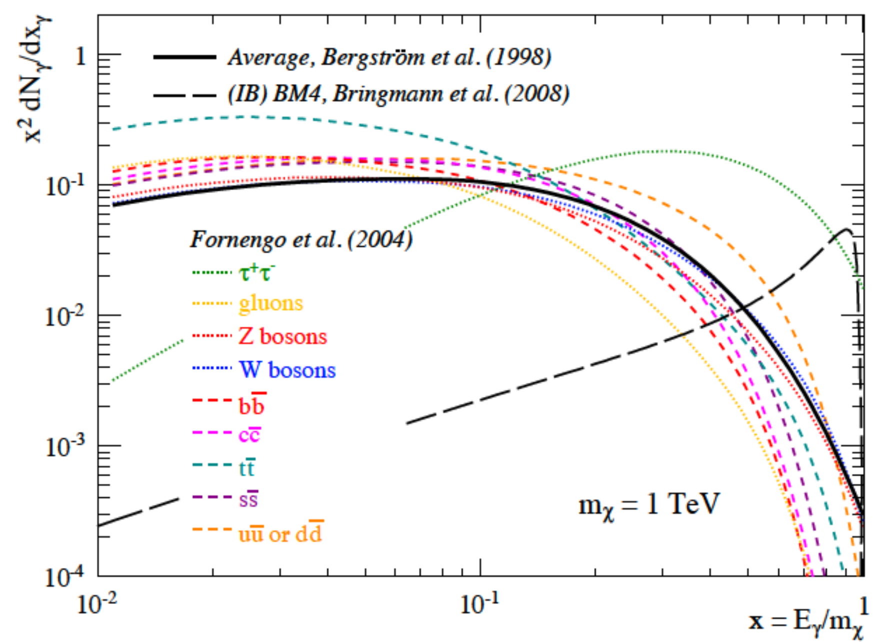

Limit on annihilation cross-section

$$\langle \sigma_{\text{ann}} v \rangle \propto m_\chi^2 \times J(\alpha_{\text{int}}) \times \text{Sensitivity} \times \frac{dN^{pp}}{dE}$$

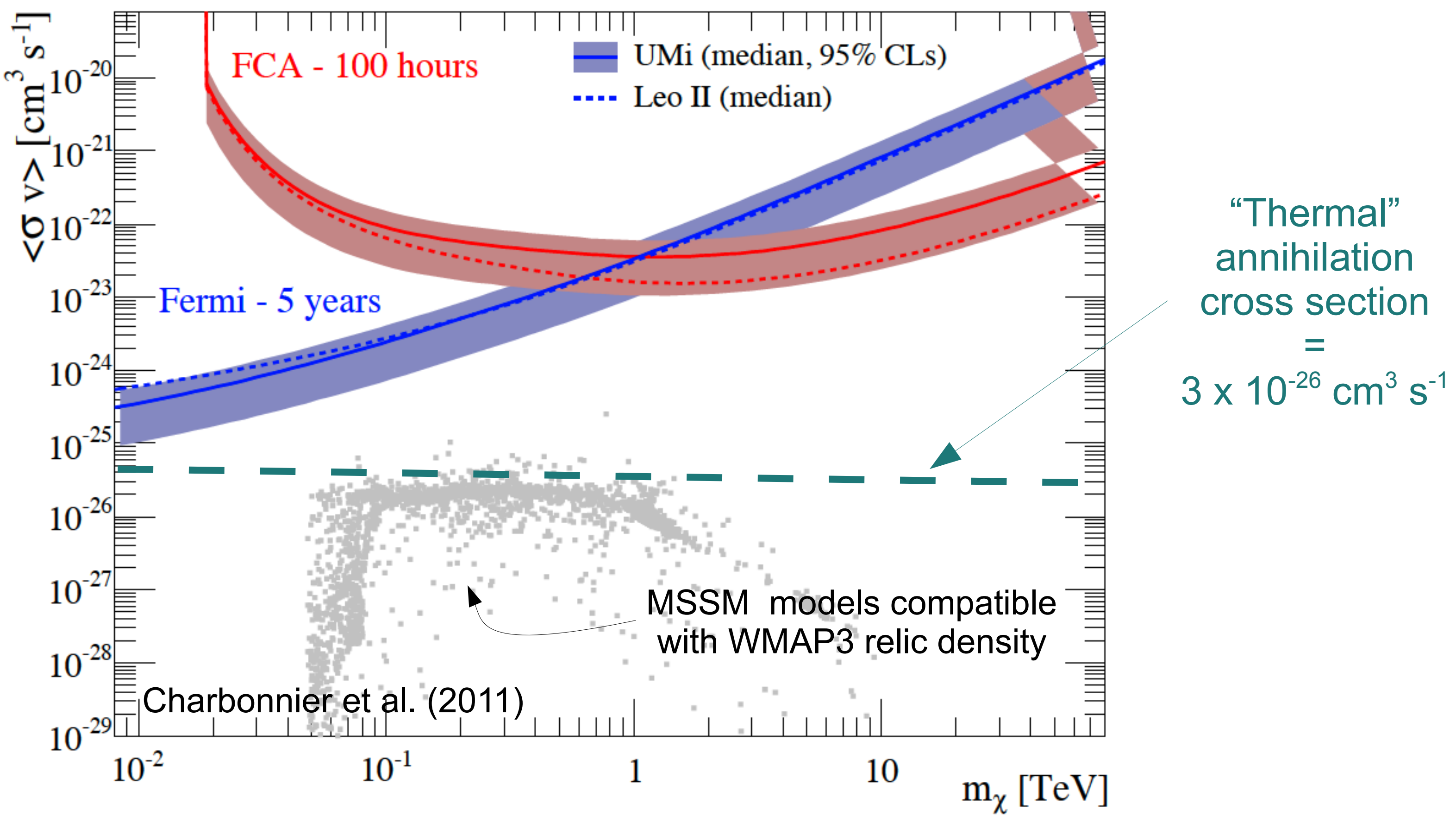

IACT current experimental status

Lamanna et al. (HESS collaboration, ICRC 2013)

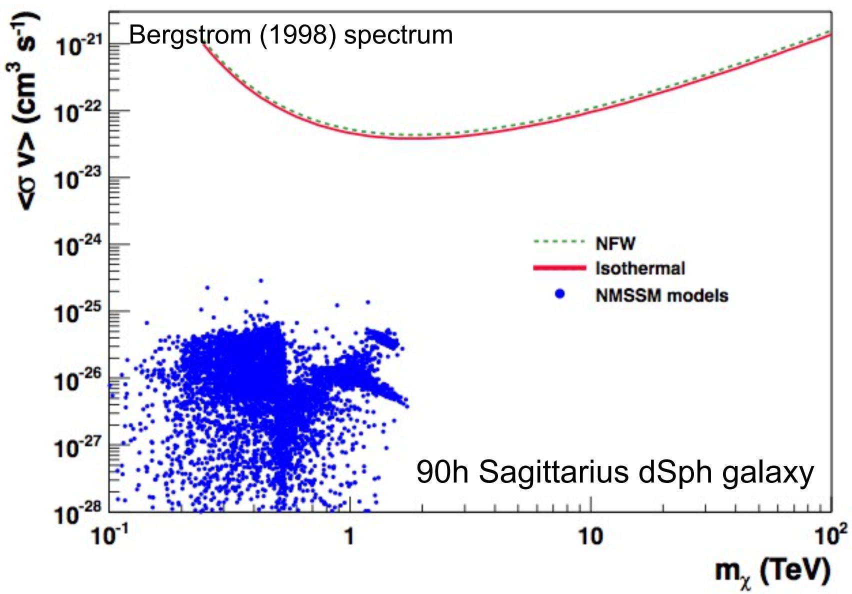

From J. Rico (MAGIC collboration)'s talk at
“What are we learning from the gamma-ray sky”
Minneapolis (October 2013)

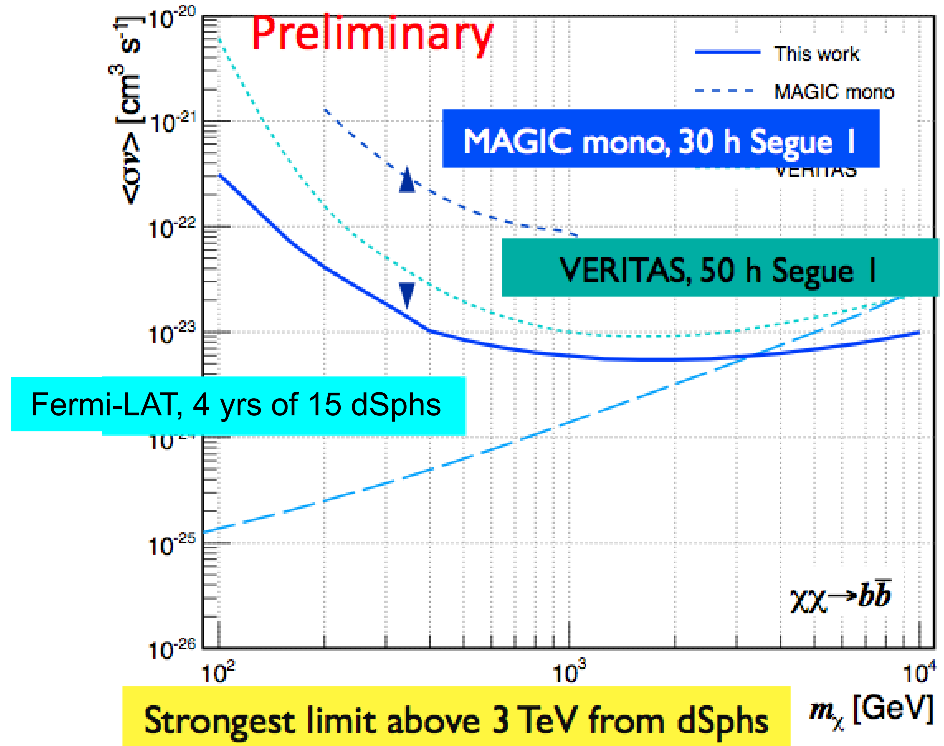

IACT are the best option from massive WIMP

Still far from “thermal” cross-section → need more sensitivity (CTA)

Fermi-LAT current experimental status

Fermi combined analysis + updated kinematics analysis

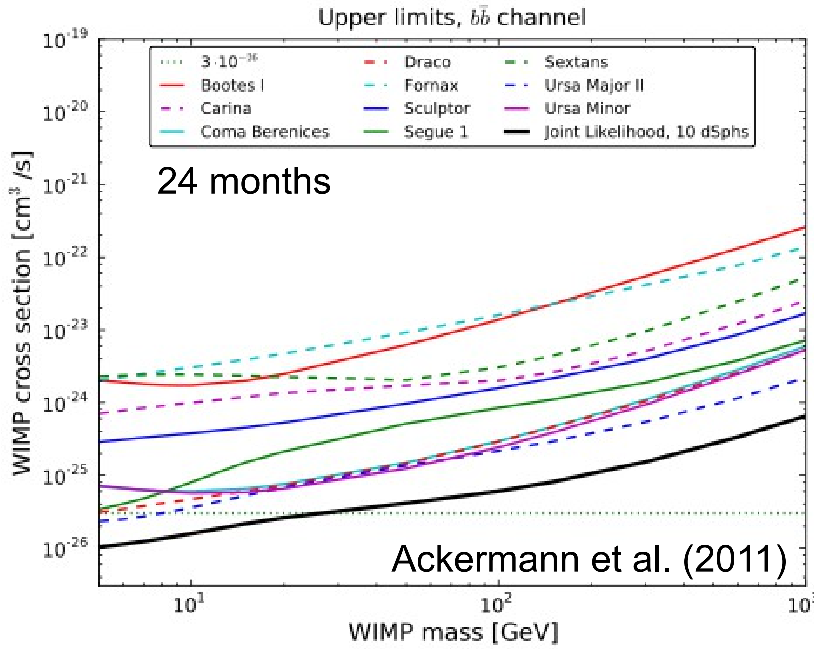

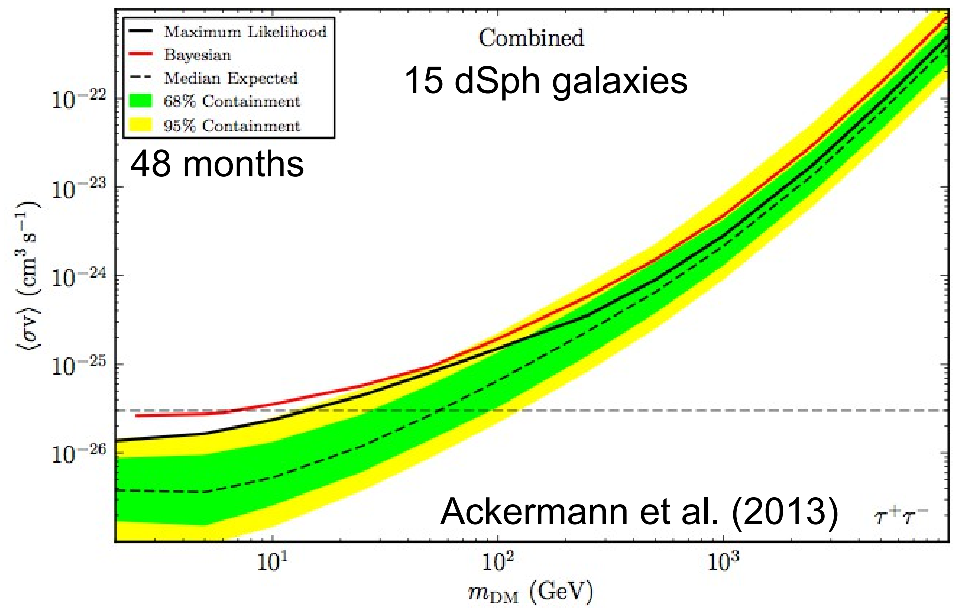

Joint likelihood allows to get better constraints

Start probing interesting region of the m - <σv> plane

Systematics in the Jeans analysis

- **Light profile and velocity dispersion**

DATA

$I(R)$ $\sigma_p^2(R)$

Deprojection - Projection

ν $\bar{v_r^2}$

- **Jean's equation: solve for $\bar{v_r^2}$**

MODEL

Stellar density *Radial velocity dispersion*

$$\frac{1}{\nu}\frac{d}{dr}(\nu\bar{v_r^2}) + 2\frac{\beta_{\rm ani}\bar{v_r^2}}{r} = -\frac{GM(r)}{r^2}$$

Anisotropy *Enclosed mass*

$$\beta_{\rm ani} = 1 - \bar{v_\theta^2}/\bar{v_r^2} \qquad M(r) = \int_0^r 4\pi s^2 \rho(s) ds$$

- **Dark matter profile**

FREE PARAM.

$$\rho(r) = \frac{\rho_s}{\left(\frac{r}{r_s}\right)^\gamma \left[1 + \left(\frac{r}{r_s}\right)^\alpha\right]^{(\beta-\gamma)/\alpha}}$$

$$\rho_s,\ r_s,\ \alpha,\ \beta,\ \gamma,\ (\text{and } \beta_{\rm ani})$$

Assumptions:

- Light profile (Plummer, cusp, etc.)
- Constant velocity anisotropy
- Choice of binning

Charbonnier et al. (2011) – test on simulated data
→ no significant impact on J-factor reconstruction

- **Spherical symmetry?**

Systematics in the Jeans analysis

Despali et al (2013)

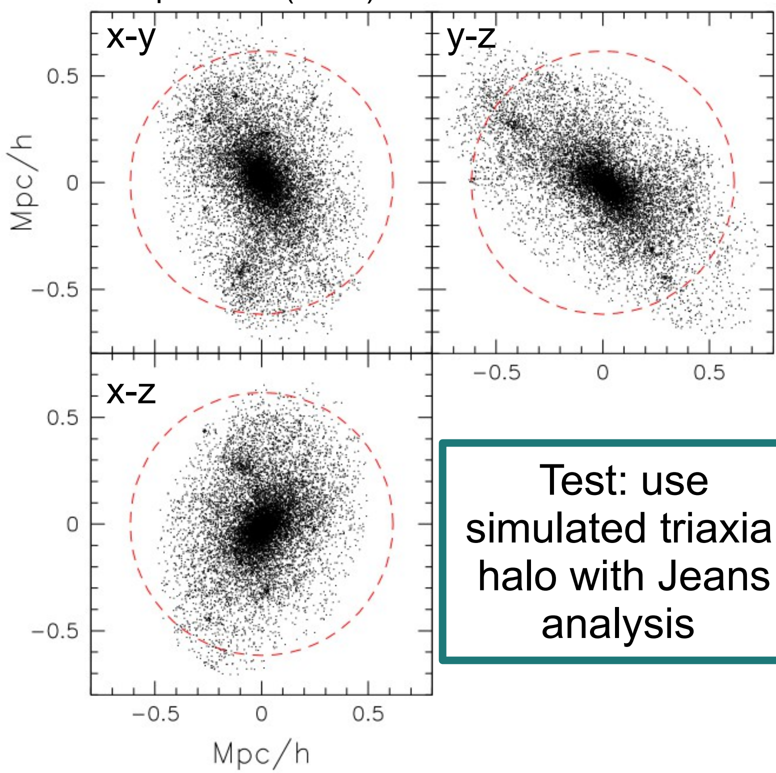

Test: use simulated triaxial halo with Jeans analysis

Haloes are triaxial

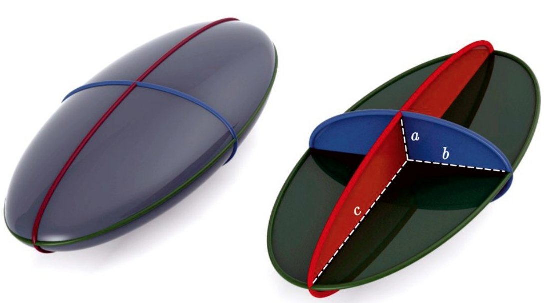

Preliminary results on triaxiality

Simulated data provided by W. Dehnen and M. Wilkinson (Univ. of Leicester)

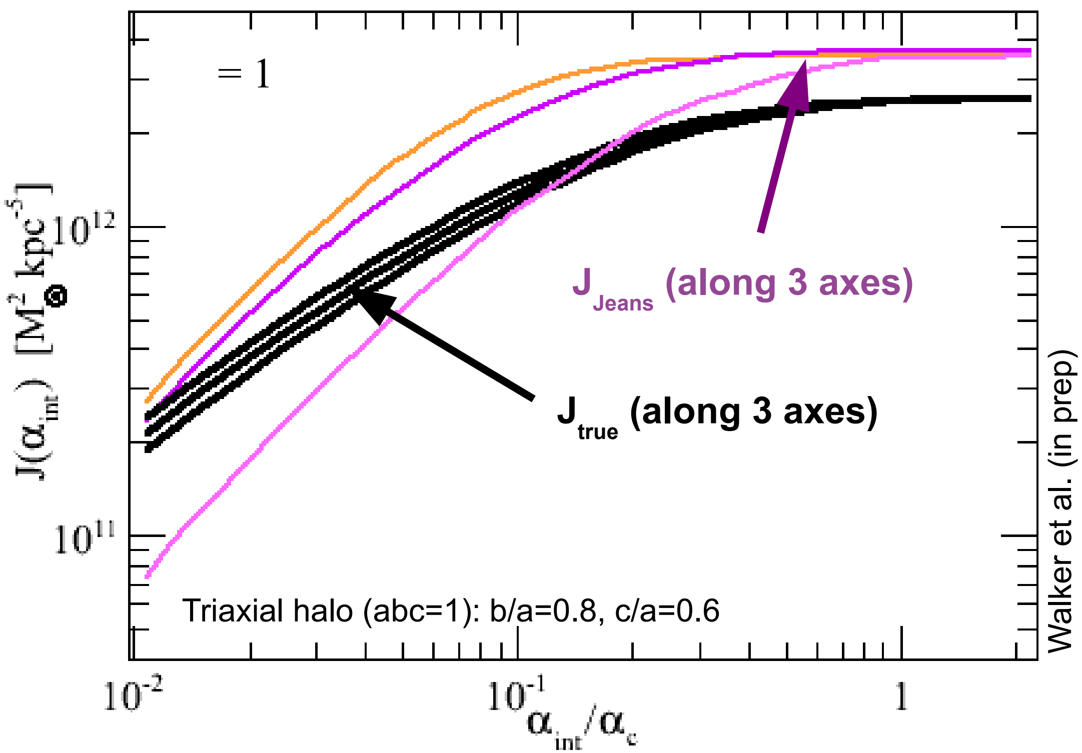

Assuming spherical symmetry has a significant impact on the J-value reconstruction

Data and methods: what's next ?

Number of position coordinates

Number of velocity coordinates

Method	Description
2+1	Only the projected radius $R^2 = x^2 + y^2$ and LOS velocity v_z is available for each star (standard technique). Large data sets (500+ stars) are currently available for the classical Milky Way dwarf spheroidal population. See the introduction for details of techniques that use 2+1 data. Standard Jeans method + higher-order Jeans method (Richardson & Fairbairn, 2013)
2+3	Proper motions of each star are added to R and v_z. This is the most likely scenario with the GAIA satellite. See Wilkinson et al. (2002), Strigari et al. (2007) and An et al. (2012) for dynamic techniques that can be applied to 2+3 data.
3+1	In this scenario the LOS depth z is available before the proper motions. This could arise if the variable nature of a star is used to determine its distance from the observer. The LOS depth can be added to R to calculate the deprojected 3D radius $r^2 = R^2 + z^2$. This is the situation that we investigate in unprecedented detail in this paper. Richardson et al.(2013)
3+3	The full 6D information of each star is known. By performing a simple coordinate transformation one has the radial and tangential velocities. The anisotropy parameter $\beta(r)$ can then be read off directly.

Richardson, Spolyar & Lehnert (2013, arXiv:1311.1522)

Dsph galaxies – summary

- DSph galaxies are interesting targets for indirect detection
- Astrophysical factor (J-factor) may be constrained from kinematic data only, using no strong prior from simulations (e.g NFW profile)
- Analysis assumes spherical symmetry → effect on triaxial halo may not be negligible
- Better data + improved methods
  → better constraints on the profiles
  → better constraints on J
  → more robust limits on annihilation cross-section

A quick introduction to indirect detection

Dwarf spheroidal galaxies: J-factor and uncertainties

Galaxy clusters: single source vs. stacking analysis

Prospects and conclusions

DM decay: Combet et al., PRD 85, 063517 (2012)
DM annihilation: Nezri et al., MNRAS 425, 477 (2012)
Disentangle DM/astro: Maurin et al., A&A 457, 16 (2012)

Galaxy clusters – observational properties

Visible

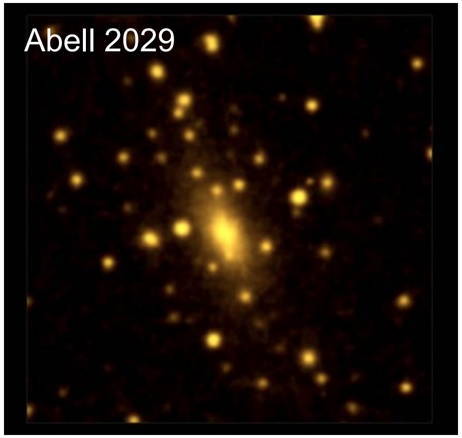

Stars/galaxies – 2%

X-ray

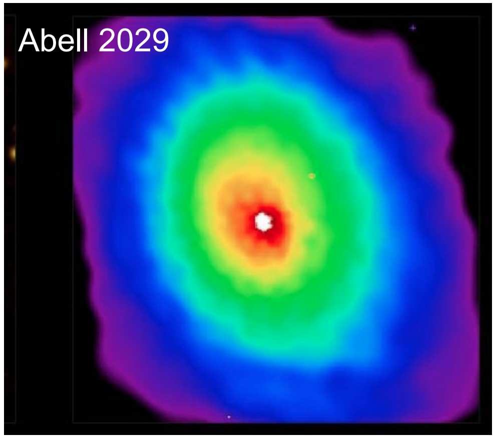

keV plasma – 13%
Intra-cluster medium (ICM)

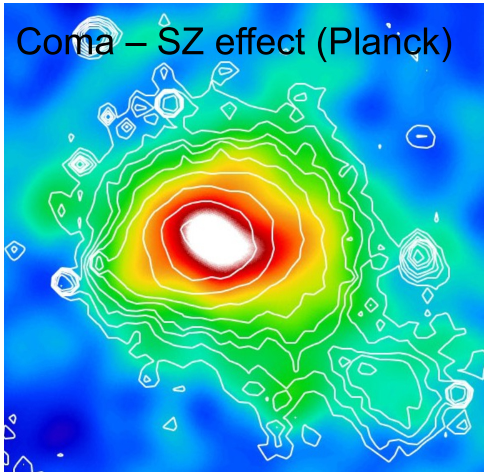

Microwave - FIR

Lensing

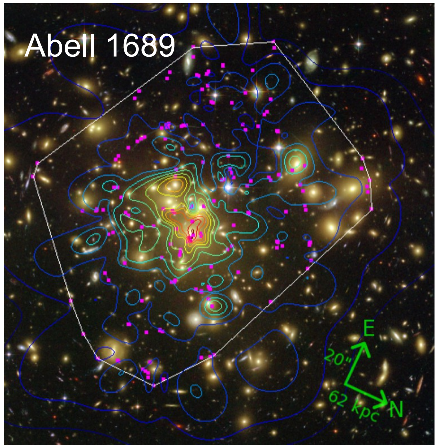

Dark matter – 85 %

Galaxy clusters – observational properties

Visible

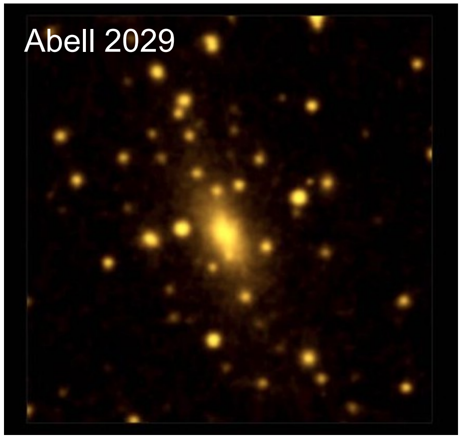

Stars/galaxies – 2%

X-ray

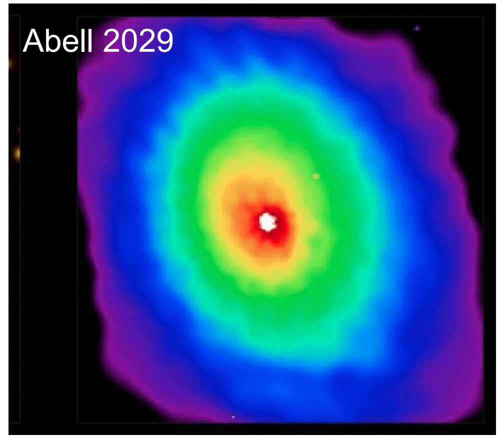

keV plasma – 13%
Intra-cluster medium (ICM)

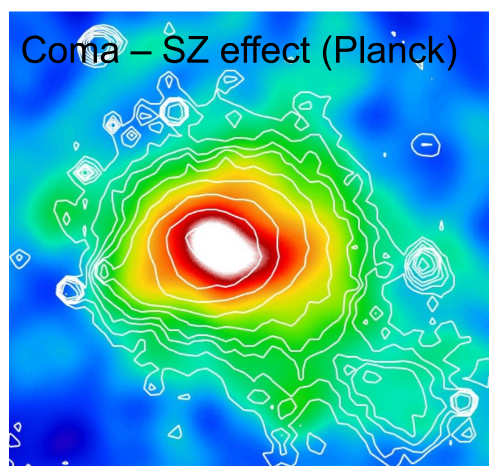

Microwave - FIR

Lensing

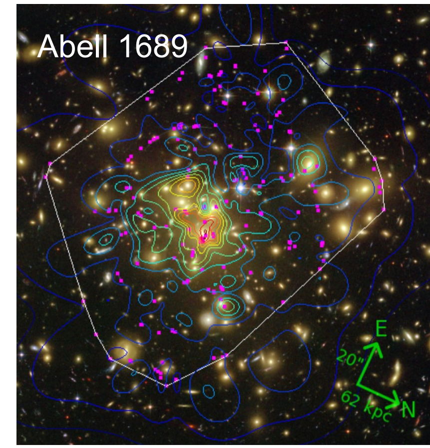

Dark matter – 85 %

Expected gamma-ray emission:

- p (CR) + p (ICM) $\rightarrow \pi^{+/-}, \pi^0 \rightarrow \gamma$
- DM annihilation/decay

DM searches in galaxy clusters

Galaxy clusters are the largest gravitationnally-bound structures in the universe, $M \sim 10^{14} - 10^{15}\ M_{sun}$ } Interesting targets for DM indirect detection

Observations

→ MAGIC: *Aleksic et al. (2010)* – Perseus

→ HESS: *Abramowski et al (2012)* – Fornax

→ Fermi*: Yuan et al. (2010), Ackermann et al. (2010), Huang et al. (2012), Zimmer et al. (2012), Ando & Nagai (2012), Han et al. (2012)*

Modelling

Jeltema et al. (2009), *Pinzke et al. (2011), Cuesta et al. (2011), Sanchez-Conde et al. (2011)*

X-ray catalogue: best up until recently, HIFLUGCS ~ 170 objects
Best targets: Coma, Fornax, AWM7, Virgo...

However, CR-induced gamma-ray signal is expected → Not ideal environments

From X-ray data to DM profile

DATA

- **X-ray observations**

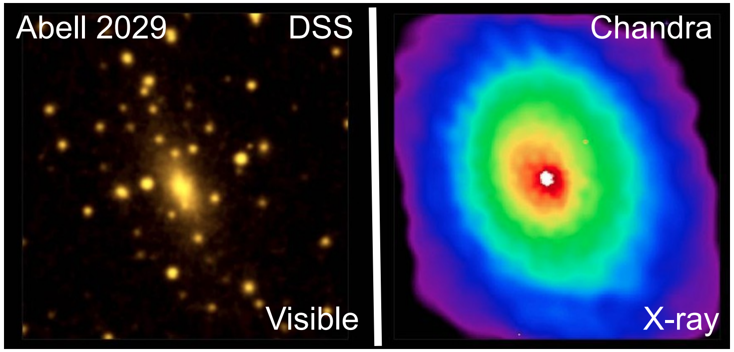

MODEL

- **Hydrostatic equilibrium**

Spher. sym. (assumed) + spectrum in shells → T(r) , ρ(r)

Assume hydrostatic equilibrium → M_{500} (< R_{500}) = f (T, ρ)

Inner slopes ∈ [0.6 – 1.9] have been inferred

(Ettori et al. 2002, Lewis et al. 2003)

PROFILE

- **Dark matter profile – NFW**

Concentration – mass relationship → $r_s = \frac{R_\Delta}{c_\Delta(M_\Delta)}$
[from N-body simus]

$$\rho(r) = \frac{\rho_s}{(r/r_s)\ [1+(r/r_s)]^2}$$ → determine ρ_s

From X-ray data to DM profile

DATA

- **X-ray observations**

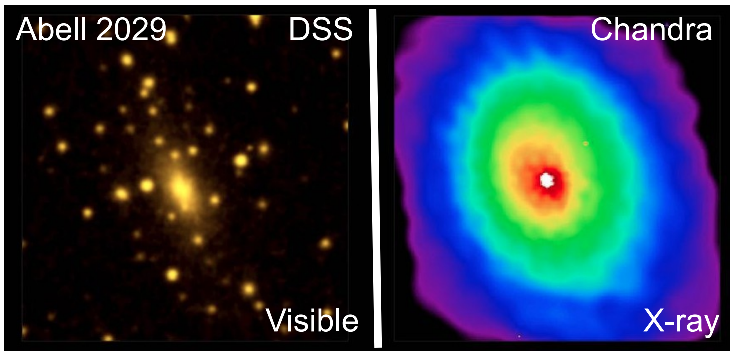

MODEL

- **Hydrostatic equilibrium**

Spher. sym. (assumed) + spectrum in shells → T(r) , ρ(r)

Assume hydrostatic equilibrium → M_{500} (< R_{500}) = f (T, ρ)

Inner slopes ∊ [0.6 – 1.9] have been inferred

(Ettori et al. 2002, Lewis et al. 2003)

PROFILE

- **Dark matter profile – NFW**

Concentration – mass relationship → $r_s = \frac{R_\Delta}{c_\Delta(M_\Delta)}$
[from N-body simus]

$$\rho(r) = \frac{\rho_s}{(r/r_s)\,\left[1 + (r/r_s)\right]^2}$$ → determine ρ_s

Meta-catalogue of 1743 X-ray clusters (<z>~0.1)

- Most data from ROSAT All Sky Survey
- Extraction and homogenisation
- Provides M_{500} and R_{500} for all objects

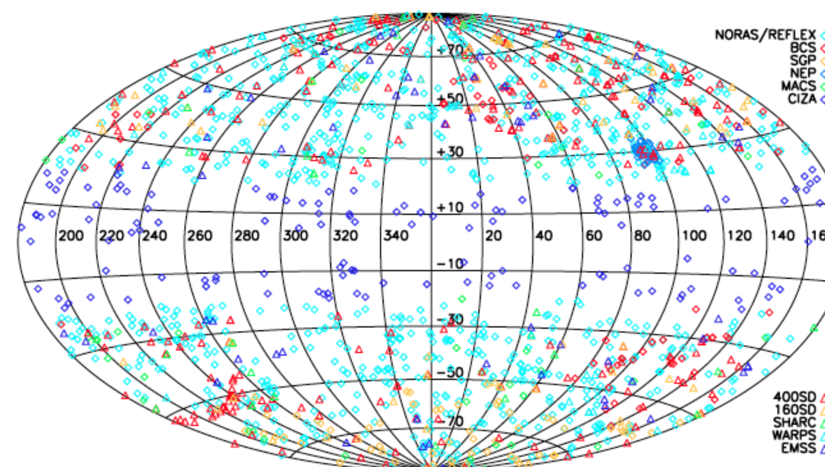

Piffaretti et al. (2011)

→ Number of objects is high enough to investigate stacking strategy

[previous studies: HIFLUGCS ~ 170 objects]
N.B.: MCXC uses improved gas distrib. w.r.t. HIFLUGCS

Ranking and contrast

$$J = \int_0^{2\pi} \int_0^{\alpha_{\rm int}} \int_0^{\infty} \rho_{\rm sm}^2 \, dl \, d\alpha \, d\beta$$

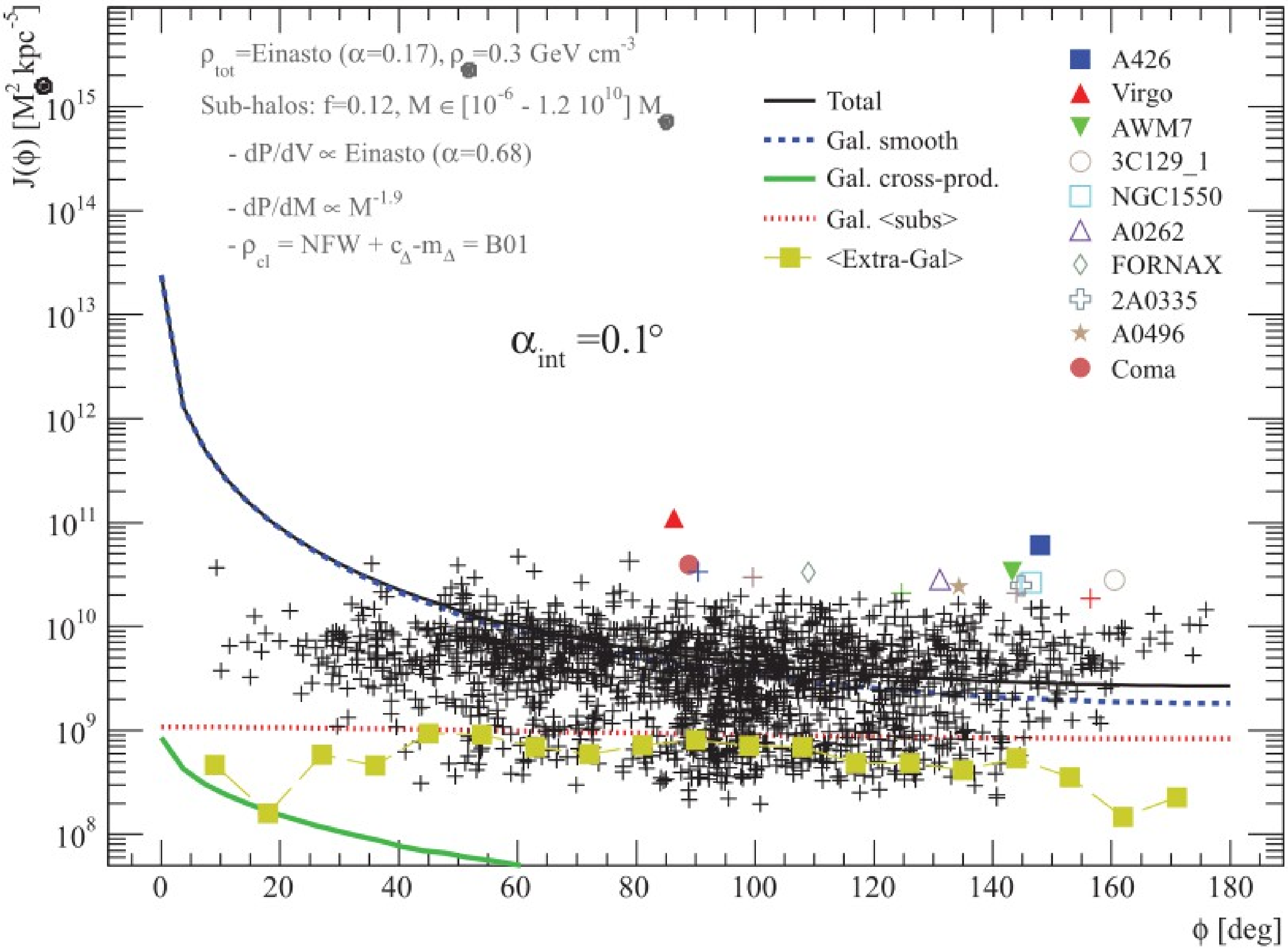

- Compromise to be found between contrast and integration angle
- By-product of analysis with MCXC (z ~ 0.1 – 0.2)

→ first data-driven lower limit on the extragalactic gamma-ray signal (J factor)

Ranking and contrast

$$J = \int_0^{2\pi} \int_0^{\alpha_{\rm int}} \int_0^{\infty} \rho_{\rm sm}^2 \, dl \, d\alpha \, d\beta$$

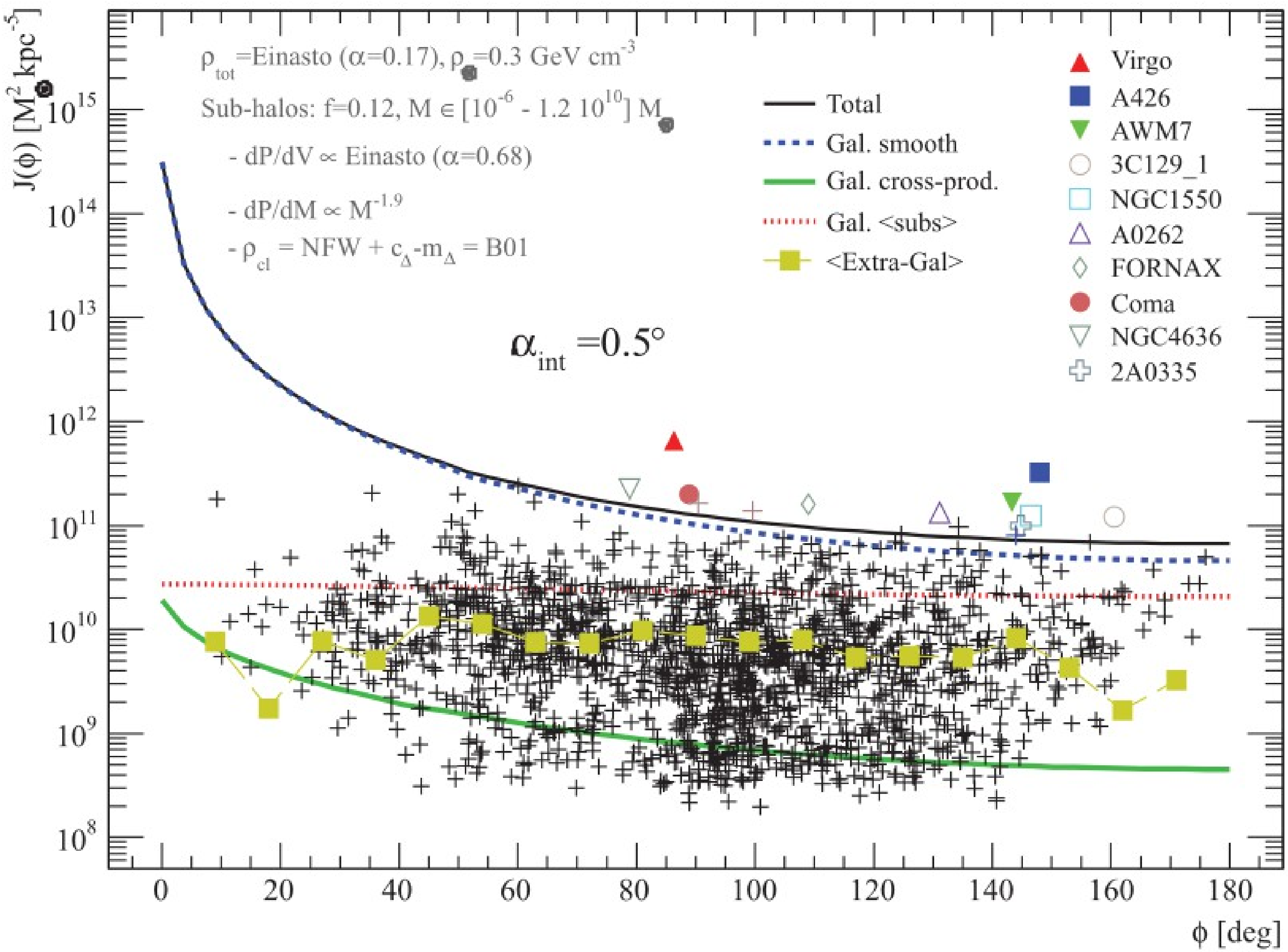

- Compromise to be found between contrast and integration angle
- By-product of analysis with MCXC (z ~ 0.1 – 0.2)

→ first data-driven lower limit on the extragalactic gamma-ray signal (J factor)

Ranking and contrast

	$\log_{10}\left(\frac{J(1^\circ)}{\mathrm{GeV}^2\ \mathrm{cm}^{-5}}\right)$				$\log_{10}\left(\frac{J(0.1^\circ)}{\mathrm{GeV}^2\ \mathrm{cm}^{-5}}\right)$	
Ref.	[1]‡	[2]§	This work		[3]¶	This work
Error	$\lesssim 0.1$	$\lesssim 0.2$	(wo/w subs)		-	(no subs)
Fornax	17.8	17.9	16.9	18.8	17.0	16.7
Coma	17.2	17.1	16.9	18.4	16.8	16.7
A1367	-	17.1	16.7	18.3	-	16.5
A1060	-	17.3	16.8	18.3	-	16.7
AWM7	17.1	17.2	16.8	18.2	-	16.6
NGC4636	17.6	17.5	17.2	18.2	-	16.9
NGC5813	-	17.3	17.1	18.1	16.4	16.8
A3526*	17.4	-	17.1	18.1	-	16.9
A426†	-	-	17.2	18.1	16.9	17.0
Ophiuchus	-	-	16.8	18.1	16.8	16.7
Virgo	-	-	17.9	18.0	17.5	17.5
NGC5846	-	-	16.7	17.9	16.5	16.5

‡Ackermann et al. (2010), §Huang et al. (2012), ¶Sánchez-Conde et al. (2011)

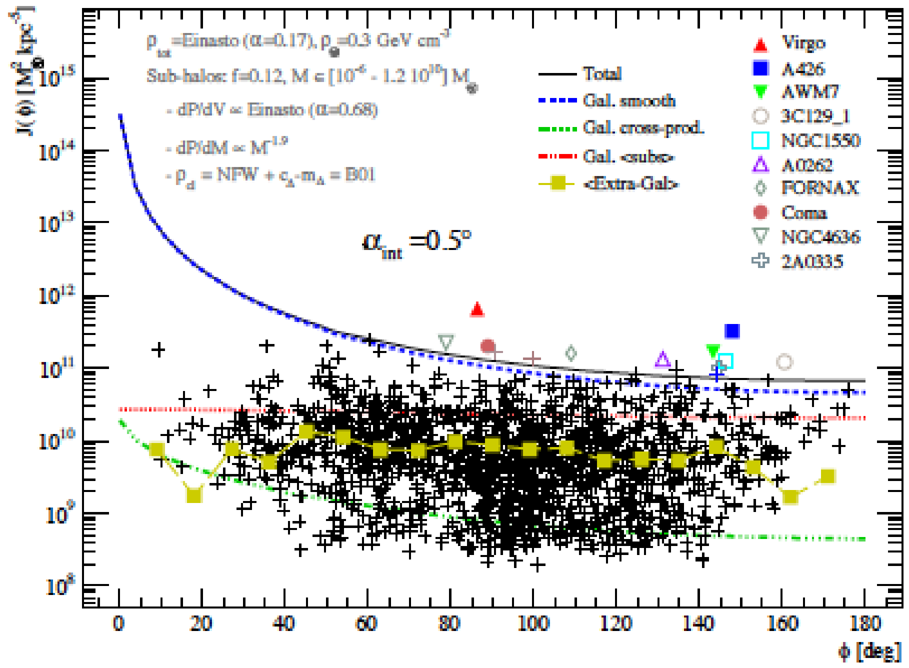

- Larger/closer clusters are favoured for single-source analysis
- Previous 'best' targets ranking based on HIFLUGCS (Sanchez-Conde et al. 2011, Pinzke et al. 2011, Gao et al 2012)

  MCXC used an improved gas description to infer M_{500}, R_{500}

J values we find from MCXC differ from previous works but should be more reliable.

J_{tot}, substructures, and boost factor

Signal boost from substructures (α_{int} vs R_{vir}/d)

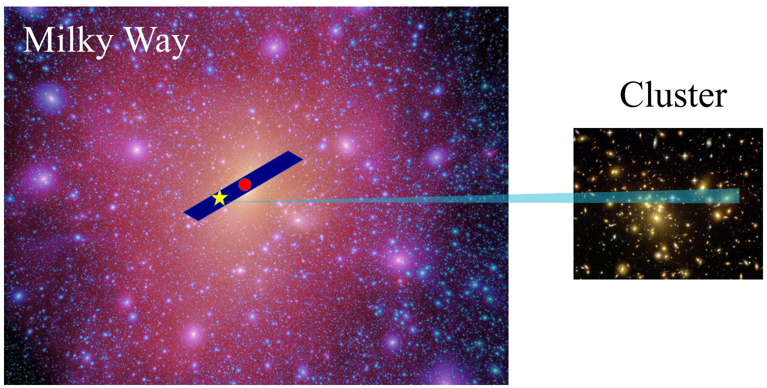

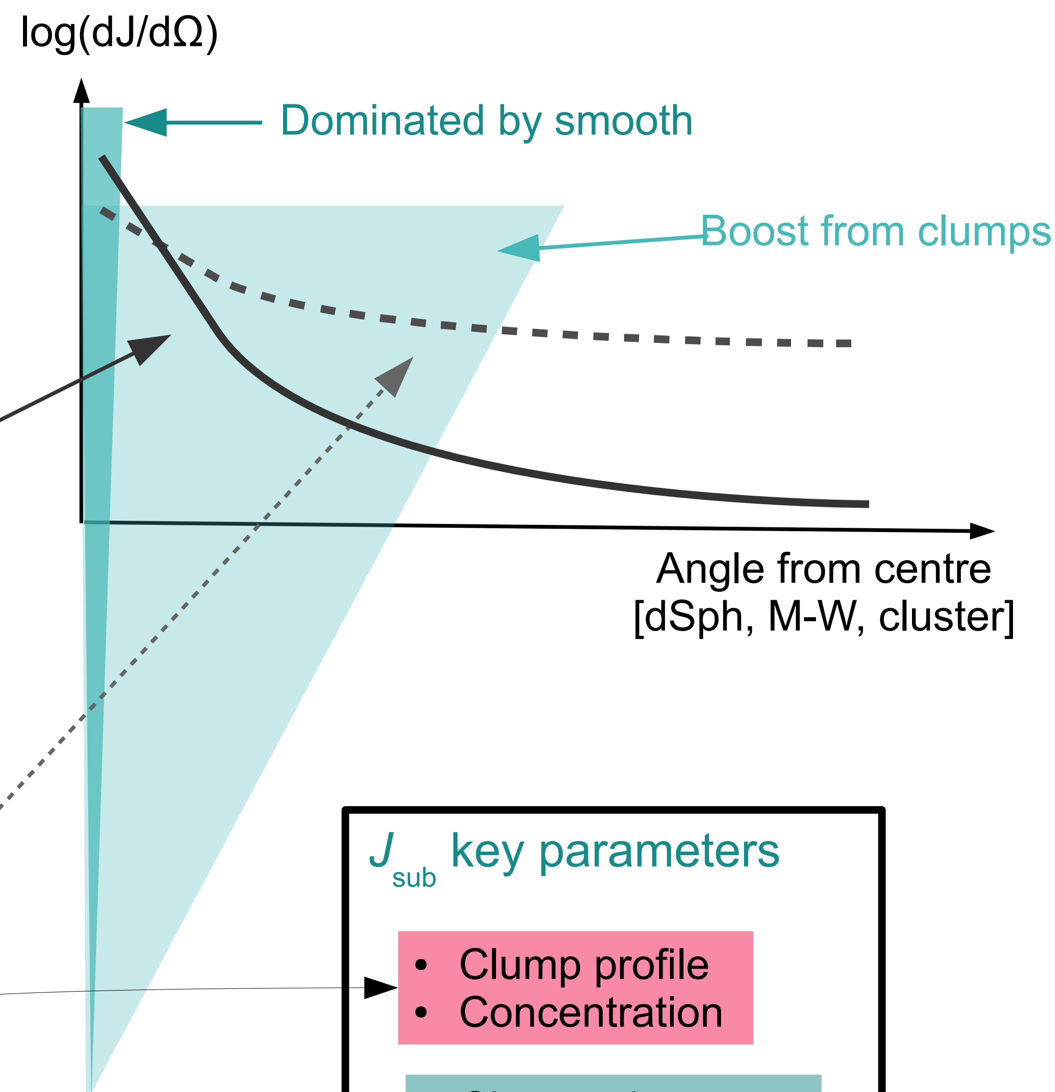

Smooth (involves $\rho_{\rm sm}^2$)

$$\frac{dJ_{\rm sm}}{d\Omega}(\theta) = \int_{l_{\rm min}}^{l_{\rm max}} \rho_{\rm sm}^2 dl$$

→ peaked near centre

Subs (involves $\rho_{\rm sub}$)
N.B.: spat. dist. flatter than $\rho_{\rm sm}$ (near centre)

$$\langle\frac{dJ_{\rm sub}}{d\Omega}(\theta)\rangle = N_{\rm tot}\int_{l_{\rm min}}^{l_{\rm max}} \frac{d\mathcal{P}_V}{dV}\int_{M_{\rm min}}^{M_{\rm max}} \mathcal{L}(M)\frac{d\mathcal{P}_M}{dM}dM$$

→ less peaked (centre), shallower decrease

J_{sub} key parameters

- Clump profile
- Concentration

- Clump min. mass
- Mass distribution

Boost factor in galaxy clusters

Varying mass distribution dN/dM + clump fraction

Reference = use Phoenix simulation
[Gao et al., MNRAS 425, 2169 (2012)]

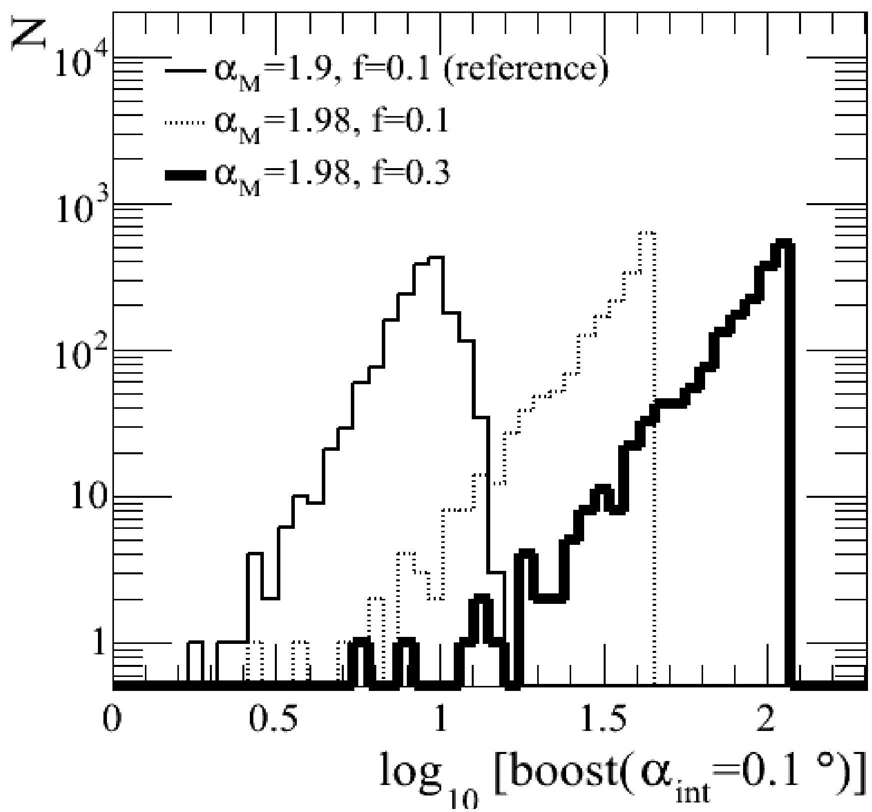

10 < Boost < 100

Substructre parameters are crucial to evaluate boost factor

Boost factor in galaxy clusters

Varying concentration

Reference = use Phoenix simulation
[Gao et al., MNRAS 425, 2169 (2012)]

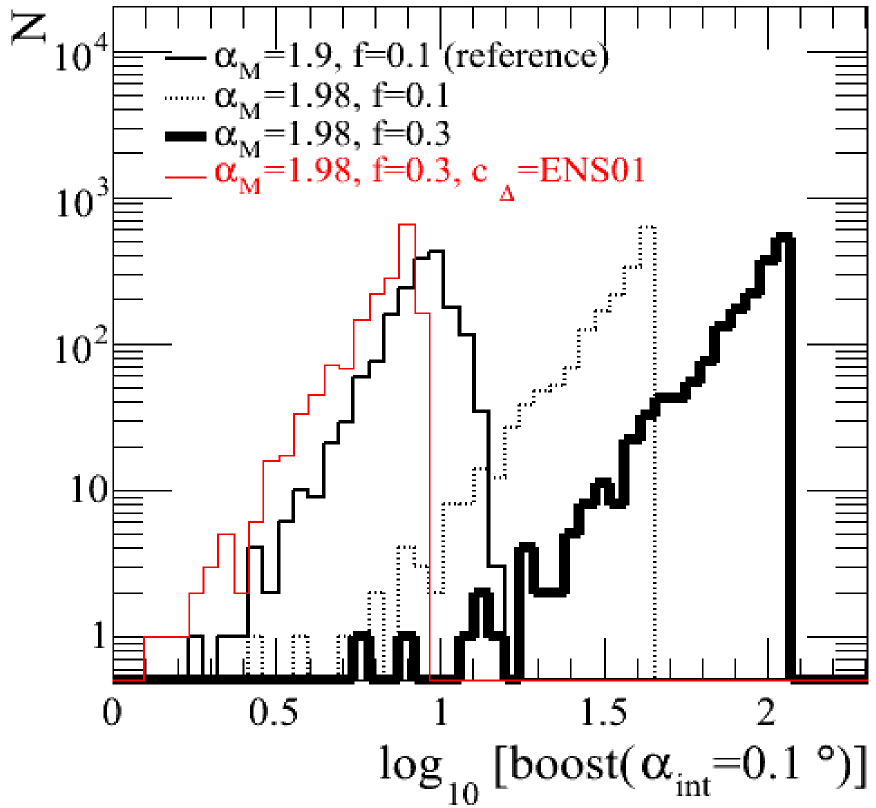

10 < Boost < 100

Boost is very sensitive to the choice of the extrapolated concentration

Boost factor in galaxy clusters

Varying the integration angle

Reference = use Phoenix simulation
[Gao et al., MNRAS 425, 2169 (2012)]

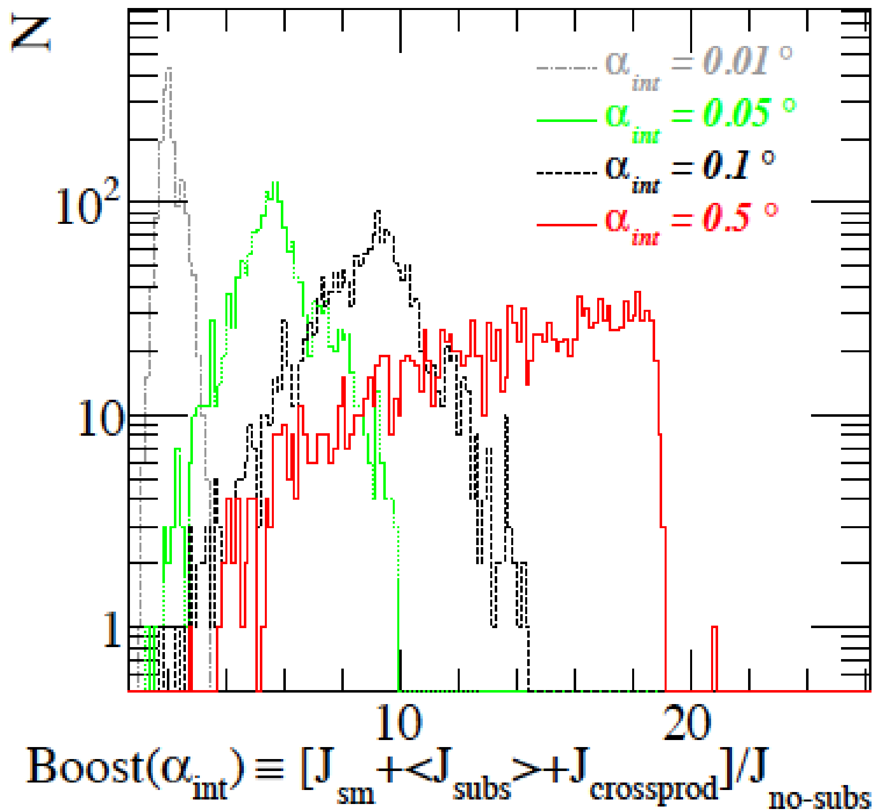

Boost from substructures of ~ 1000 are excluded
→ confirmed by Sanchez-Conde & Prada (in prep)

Current experimental limits

Abramowski et al. (HESS collabortion, 2012)

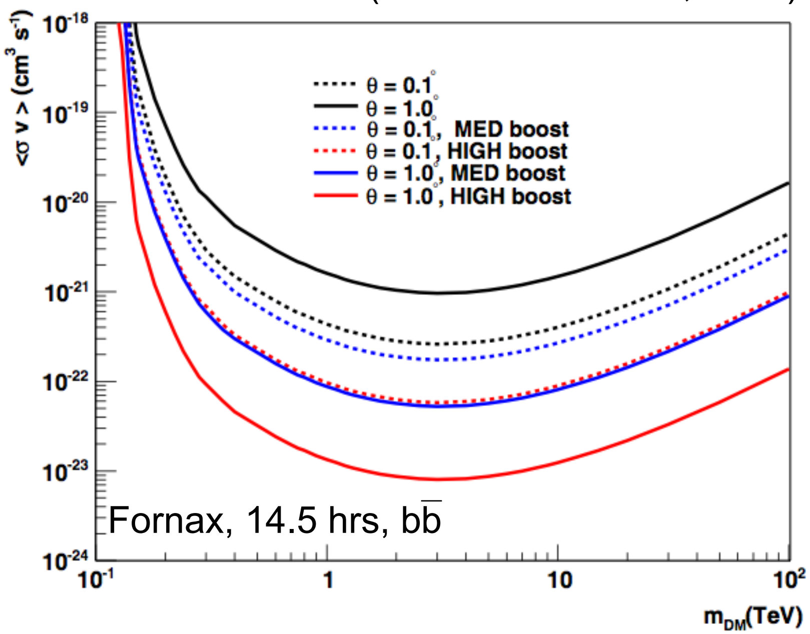

Arlen et al. (VERITAS collabortion, 2012)

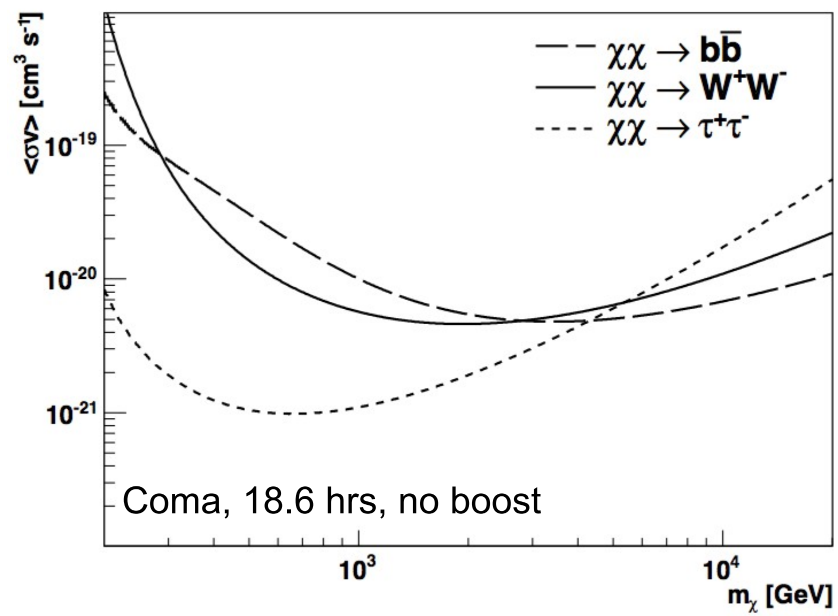

Zimmer, Conrad & Pzinke (Fermi-LAT collabortion)

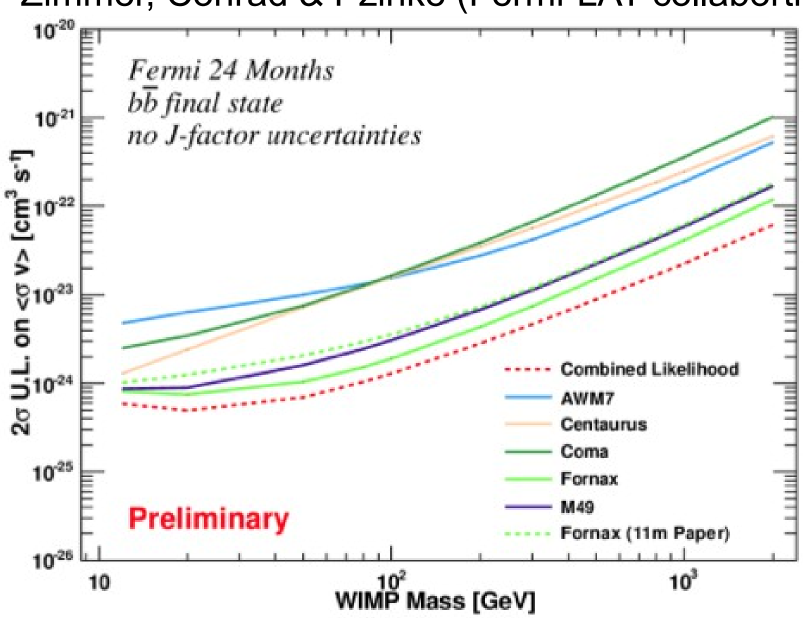

Limit not as good as that from dSph galaxies

Is it possible to improve on the single-source approach using a stacking strategy?

Stacking for galaxy clusters, naively

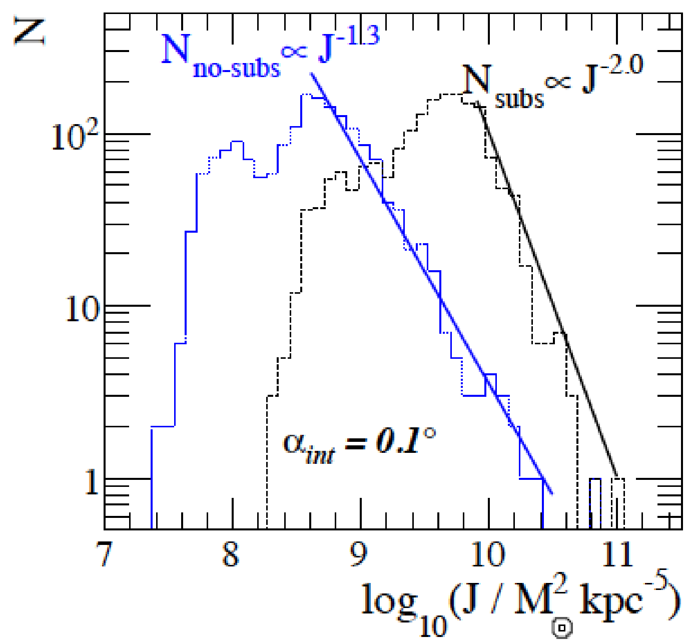

Annihilation:

- If no clumps → stacking is pointless
- With substructures → stacking could be interesting as

100 times more objects at J/10
(for our reference substructure configuration)

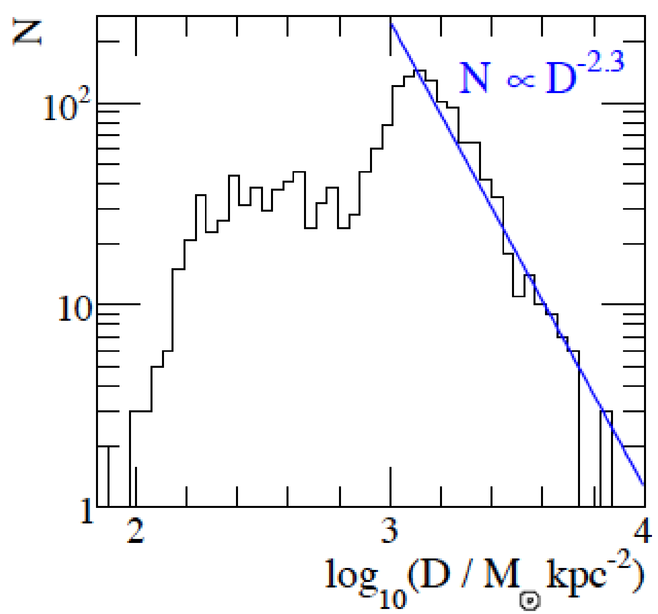

Decaying DM → stacking also looks promising

But need consider instrumental response
and observation strategy
→ Answer depends on type of detector

Stacking for galaxy clusters

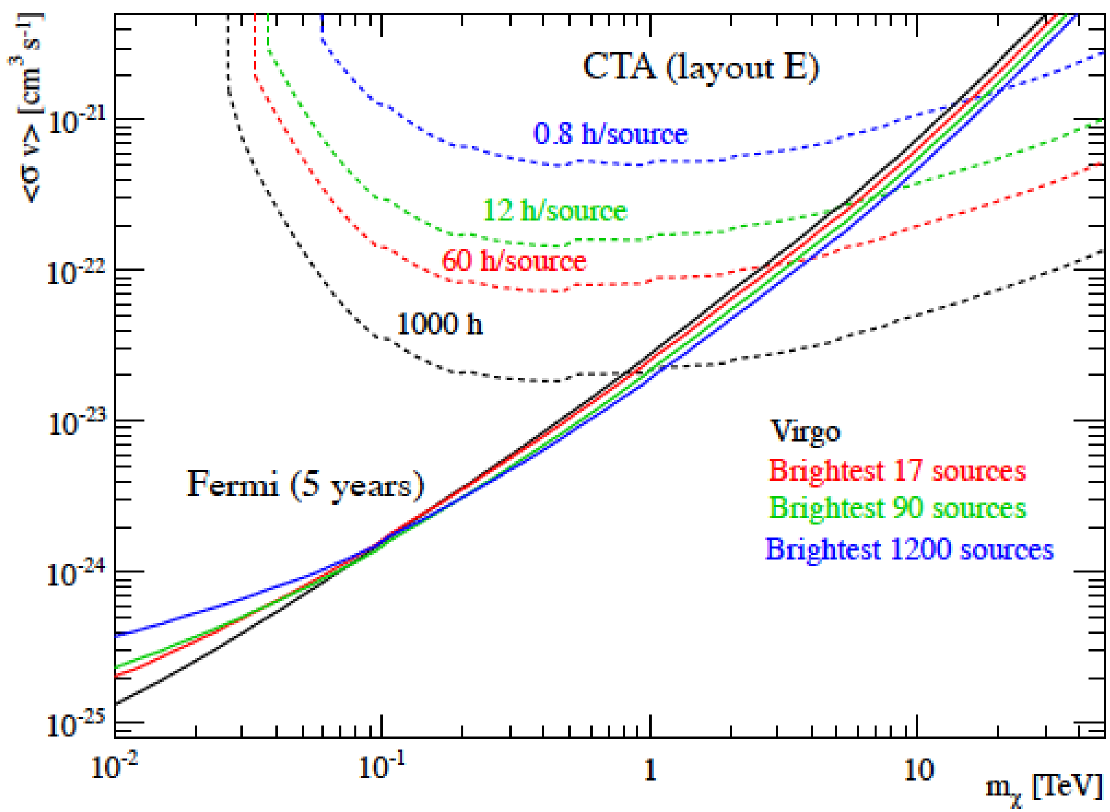

→ CTA: stacking worsens prospects (need to adapt total observation time to each source)

→ Fermi-LAT: slight improvement (~1.7) > 0.1 TeV (poor resolution = no benefit at low E)

Stacking for galaxy clusters

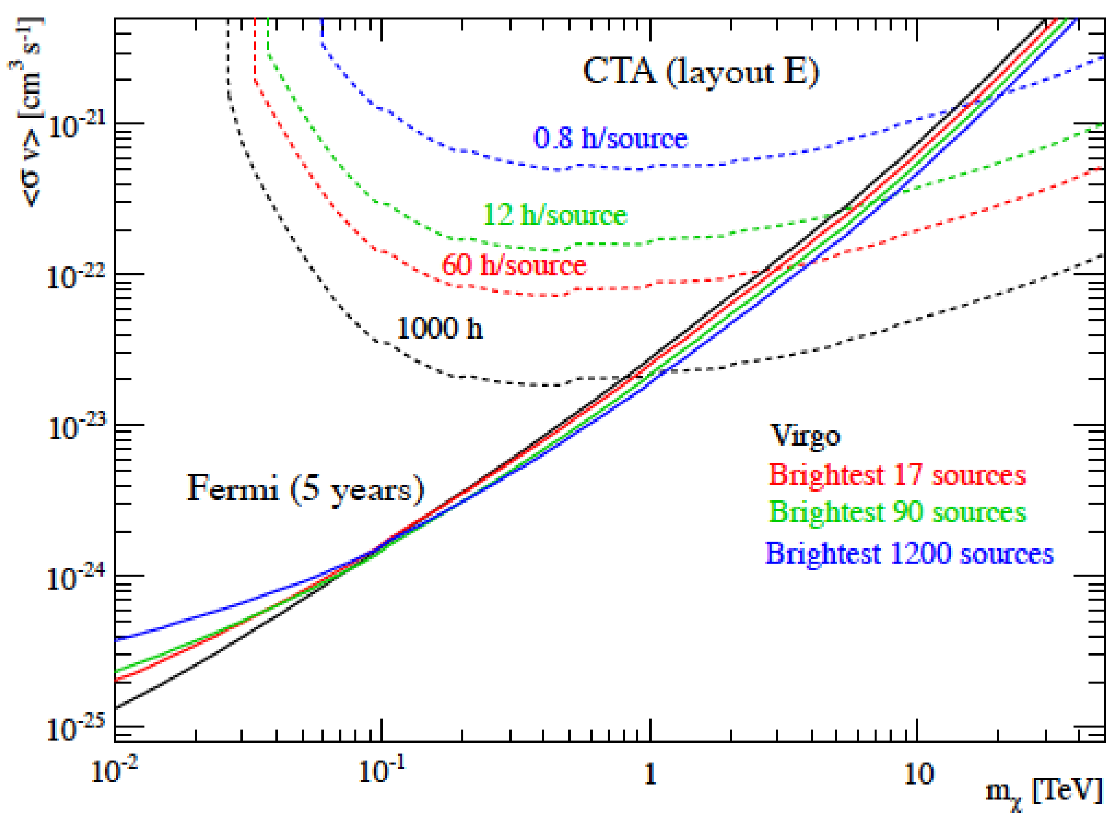

→ CTA: stacking worsens prospects (need to adapt total observation time to each source)

→ Fermi-LAT: slight improvement (~1.7) > 0.1 TeV (poor resolution = no benefit at low E)

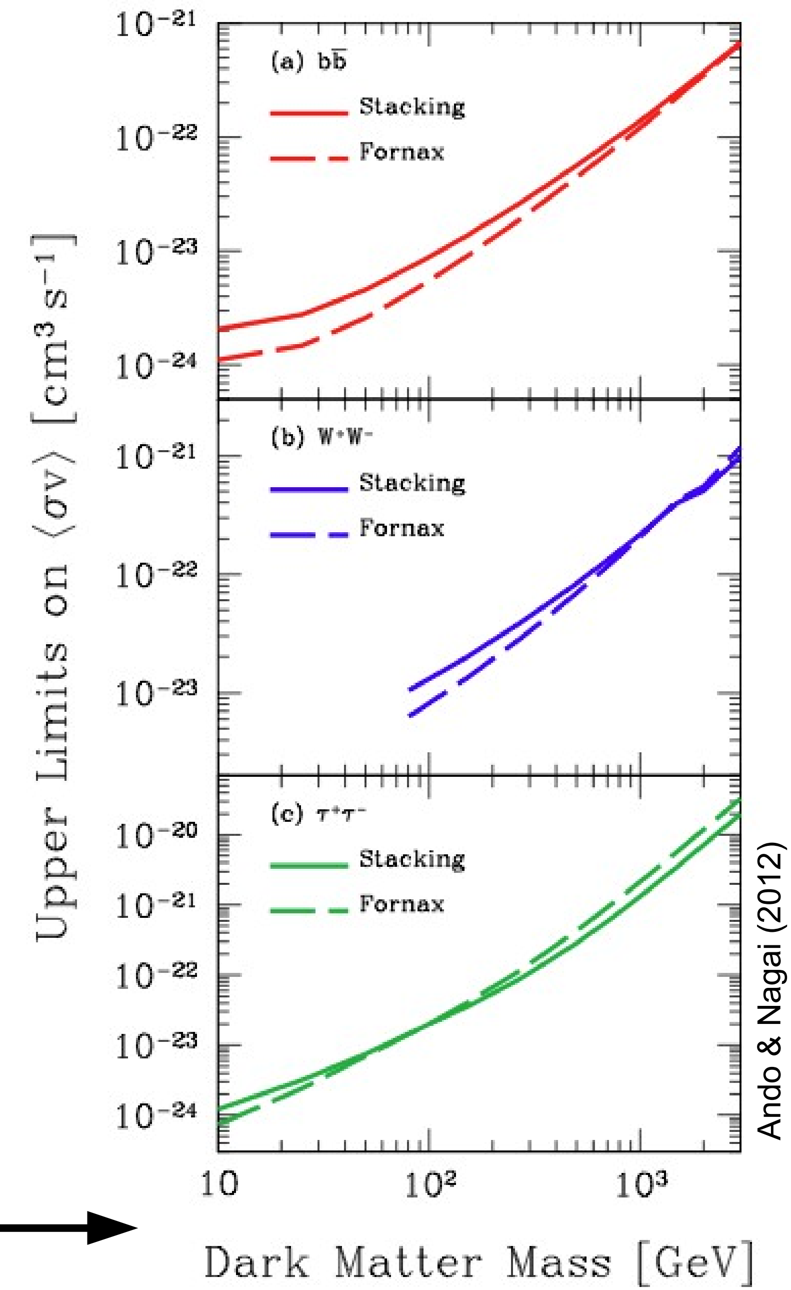

Confirmed by independent work by Ando & Nagai (2012)
2.8 yrs Fermi data – 49 'nearby massive clusters' →

A quick introduction to indirect detection

Dwarf spheroidal galaxies: J-factor and uncertainties

Galaxy clusters: single source vs. stacking analysis

Prospects and conclusions

DSph galaxies or galaxy clusters?

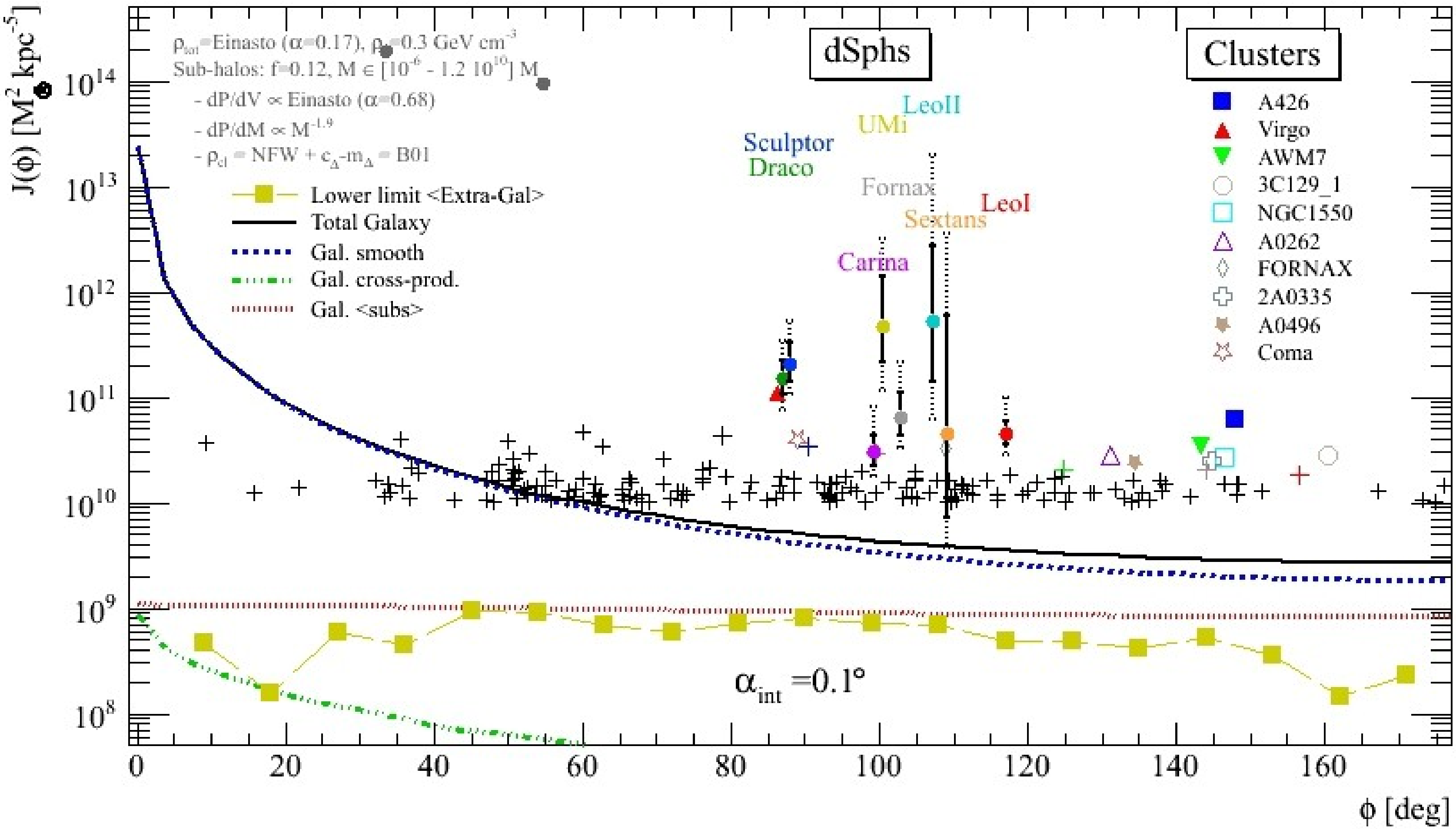

DSph galaxies are a better option (larger J, no bkgd, robust)
+ more data expected for ultra-faint dSph galaxies
+ more ultra-faint dSph galaxies should be discovered (LSST)

Galaxy clusters interesting because of their astro. background

Overall picture

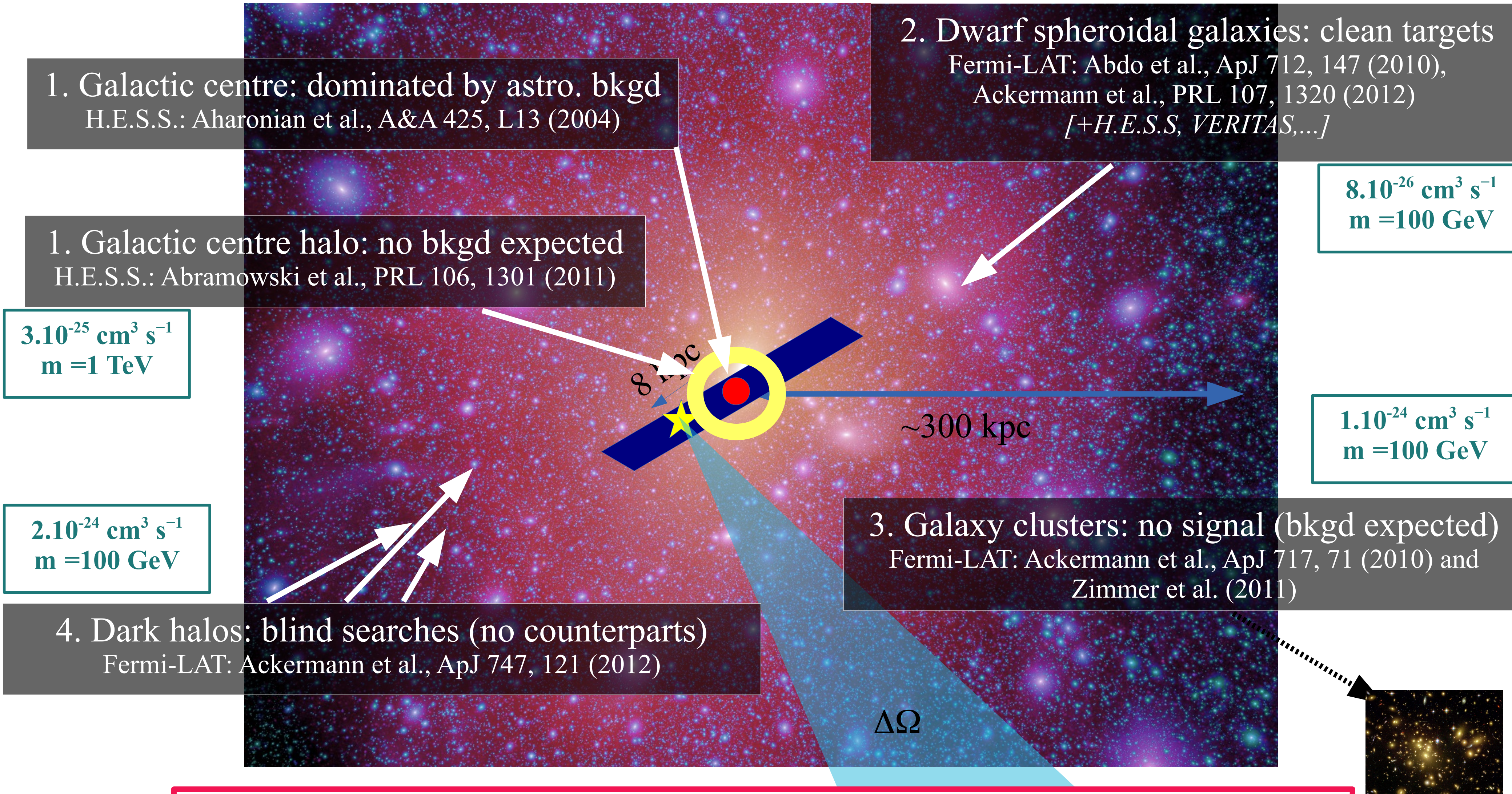

We are only starting to reach interesting <σv> regions of DM parameter space